Contract No:

This document was prepared in conjunction with work accomplished under Contract No. 89303321CEM000080 with the U.S. Department of Energy (DOE) Office of Environmental Management (EM).

Disclaimer:

Survey of U.S. Research Reactor Auxiliary Facilities Used for Material Testing and Basic Neutron Science

PRO-X-2023-004
SRNL-TR-2023-00298

Prepared by N. Groden, C. Sobecki, J. Kinyon, N. Drey, C. Verst, S. Peters, C. Nicholson, R. Sindelar, and D. Vinson

Office of Conversion
Material Management and Minimization Program
Office of Defense Nuclear Nonproliferation
National Nuclear Security Administration
U.S. Department of Energy

31 May 2023

Executive Summary

A catalogue of and attributes of the Materials Irradiation and Testing facilities (MIF) and the Basic Neutron Science facilities (BSF) of auxiliary (AUX) facilities of research reactors are compiled. The survey of these facilities is drawn from the set of U.S. university and DOE research reactor facilities and should be considered as a reference point when comparing commonalities in international AUX facilities. The size and shielding capabilities of the facilities, the typical characterization equipment used, and the neutron flux and irradiation capabilities of the facilities are listed. Short descriptions of experimental activities and current practices are detailed for MIFs and BSFs.

The attributes are important in consideration of the reconfiguration of the facilities for purposes other than stated mission, i.e., for proliferation of weapons-usable nuclear material (WUNM). An evaluation of the capacity for production rate of WUNM from neutron beams-on-targets or a sample that has been placed in an irradiation position for a period is provided.

Further evaluation of reconfiguration of these MIF and BSF are recommended to refine the proliferation risks. Specifically, MIF hot cells and potential configurations, additional modeling of facility throughput and development of methods for determining levels of concern for MIF and BSF have all been identified as steps for refinement of determination of the risks associated with these facilities. Future work will focus on:

1. A model of projected throughput for different MIF and BSF configurations that will be used to provide a window of potential operational misuse for a facility and better understand the capability of production and the rate of processing for WUNM in these facilities.
2. A misuse study for various configurations of MIF hot cell layouts detailing capacity, specifications, shielding constraints for MIF operations, identification of a maximum shielding thickness, and reasonable need associated with each activity performed in a MIF.
3. Development of a rule of thumb rating system utilizing data gathered from previous reports to show levels of concern at a given power level, flux, and experiment set.

Table of Contents

List of Tables

List of Figures

List of Acronyms

Acronym	Definition
ANL	Argonne National Laboratory
AUX	Auxiliary Capabilities
BSE	Back-Scattered Electrons
BSF	Basic Science Facility
DOE	Department of Energy
DSC	Differential Scanning Calorimetry
DU	Depleted Uranium
EBSD	Electron Backscatter Diffraction
EDS	Electron Dispersive Spectroscopy
EELS	Electron Energy Loss Spectroscopy
EML	Electron Microscopy Lab
EPMA/EMPA	Electron Probe Microanalysis / Electron Microprobe Analysis
FASB	Fuels and Applied Science Building
FIB	Focused Ion Beam
HFEF	Hot Fuel Examination Facility
HFIR	High Flux Isotope Reactor
HLRF	High Level Radiochemistry Facility
IFEL	Irradiated Fuels Examination Laboratory
IMCL	Irradiated Materials Characterization Laboratory
IMET	Irradiated Material and Examination Testing
IML	Irradiated Materials Laboratory
INL	Idaho National Laboratory
LA-ICPMS	Laser-Ablation Inductively Coupled Plasma Mass Spectroscopy
MEC	Materials Examination Cell
MIF	Materials Irradiation Facility
MITR	Massachusetts Institute of Technology Reactor
MOX	Mixed-Oxide
NAA	Neutron Activation Analysis
NRAD	Neutron Radiography
NRC	Nuclear Regulatory Commission
ORNL	Oak Ridge National Laboratory
PGET	Passive Gamma Emission Scanning Tomography

PIE	Post-Irradiation Examination
PNNL	Pacific Northwest National Laboratory
PRO-X	Proliferation Resistance Optimization
RPL	Radiochemical Processing Laboratory
RR	Research Reactor
SAL	Shielded Analytical Laboratory
SE	Secondary Electron
SEM	Scanning Electron Microscopy
SIMS	Secondary Ion Mass Spectrometry
SNM	Special Nuclear Materials
SRNL	Savannah River National Laboratory
STEM	Scanning Transmission Electron Microscopy
TEM	Transmission Electron Microscopy
TGA	Thermogravimetric Analysis
WDS	Wavelength Dispersive Spectroscopy
WUNM	Weapons-Useable Nuclear Material
XAFS	X-ray Absorption Fine Structure
XAS	X-ray Absorption Spectroscopy
XRD	X-ray Diffraction
XRF	X-ray Fluorescence

1. Introduction

The "Proliferation Resistance Optimization" (PRO-X) program provides a framework for research reactor (RR) system designs that maximizes performance for stated peaceful uses and minimizes special nuclear materials (SNM) (i.e., U, Pu, tritium, etc.) usage, productions, and diversion pathways. PRO-RR can be broken down into three technical areas: Core Design, Fuel Design and Fabrication, and Auxiliary Capabilities. The generic scope of these technical areas is illustrated by Figure 1-1.

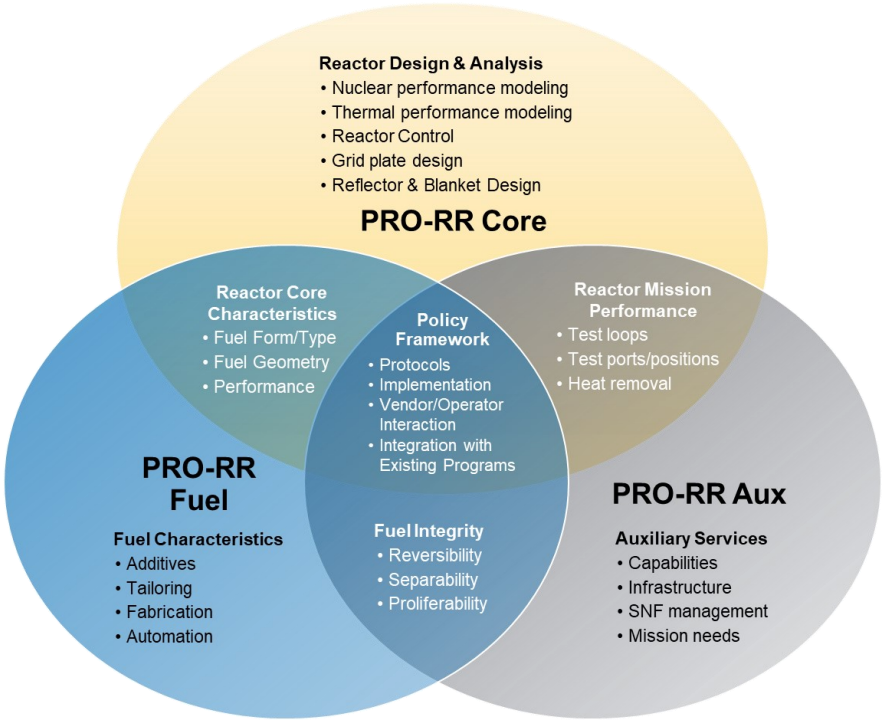

Figure 1-1: Venn diagram of PRO-RR technical areas scope.

The PRO-RR program is dedicated to optimizing the proliferation resistance of research reactors, and the Auxiliary facilities (AUX) team focuses on support structures defined as any physical facility that enable capabilities beyond that of a typical research reactor. As one of the initial steps in the PRO-X Multivariate Optimization approach for AUX (Figure 1-2), this report details two of the three main AUX facility types that support research reactors.

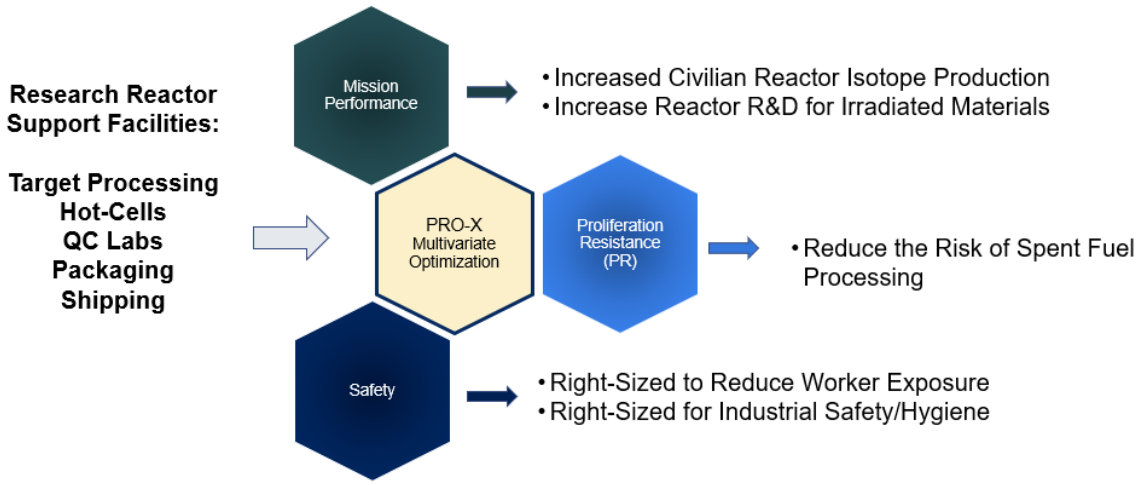

Figure 1-2: PRO-X optimization strategy balances performance of a research reactor with proliferation resistance and enhanced safety.

This report serves as a survey of the commonalities between specific auxiliary facility designs for materials irradiation and neutron sciences using references acquired from national laboratory and university reporting. To perform this survey, AUX facilities supporting RR in the United States were used as a basis of comparison between AUX facilities. U.S. RR AUX facilities were also chosen due to the wealth of information available for these facilities. Section 2 describes typical attributes among AUX facilities, Sections 3 and 4 divide facilities between material irradiation capabilities and basic sciences. Section 5 discusses proliferation concerns and opportunities for optimization within auxiliary facilities. Section 6 makes conclusions on the selected auxiliary facilities found in the U.S. and presents a pathway for future work.

2. Typical Attributes of AUX Facilities

As of June 2021, the IAEA determined that there were 223 active research reactors in over 30 different countries across the world, of which there are 50 in the United States. In addition to these RRs, fuel is provided to many RRs around the world by the U.S. Thus the U.S. provides a large amount of data and methodology to inform and develop international AUX facilities. Auxiliary facilities that support a nuclear program, however, are some of the most diverse portions of a nuclear site. Due to the complexity of a purpose-built RR facility, processes, equipment, and capabilities can be wildly different between programs. Despite this, commonalities between RR programs exist and apply to most facilities at differing levels depending on the stated purpose of the program.

Three general categories of auxiliary facilities are considered based on capabilities to be provided: Isotope Production; Materials Irradiation and Testing; and Neutron Science. Isotope production facilities typically deal with processing of radiological isotopes for medical or industrial applications and include hot cells with chemical separation equipment. Materials irradiation and neutron optical science facilities involve specific support equipment that enables neutron radiation generated at the core of the reactor to interact with test materials. After irradiation of the material, that material is either processed for qualification using a Post Irradiation Examination (PIE) technique or is analyzed to characterize properties of the irradiated material. The AUX facilities of a RR have been divided into Isotope production facilities, material

irradiation and testing facilities (MIFs) and basic science facilities (BSFs) (Figure 2-1) depending on the type of work the facility is dedicated to. Details on isotope production facilities are described in separate topical reports prepared under the PRO-X program.

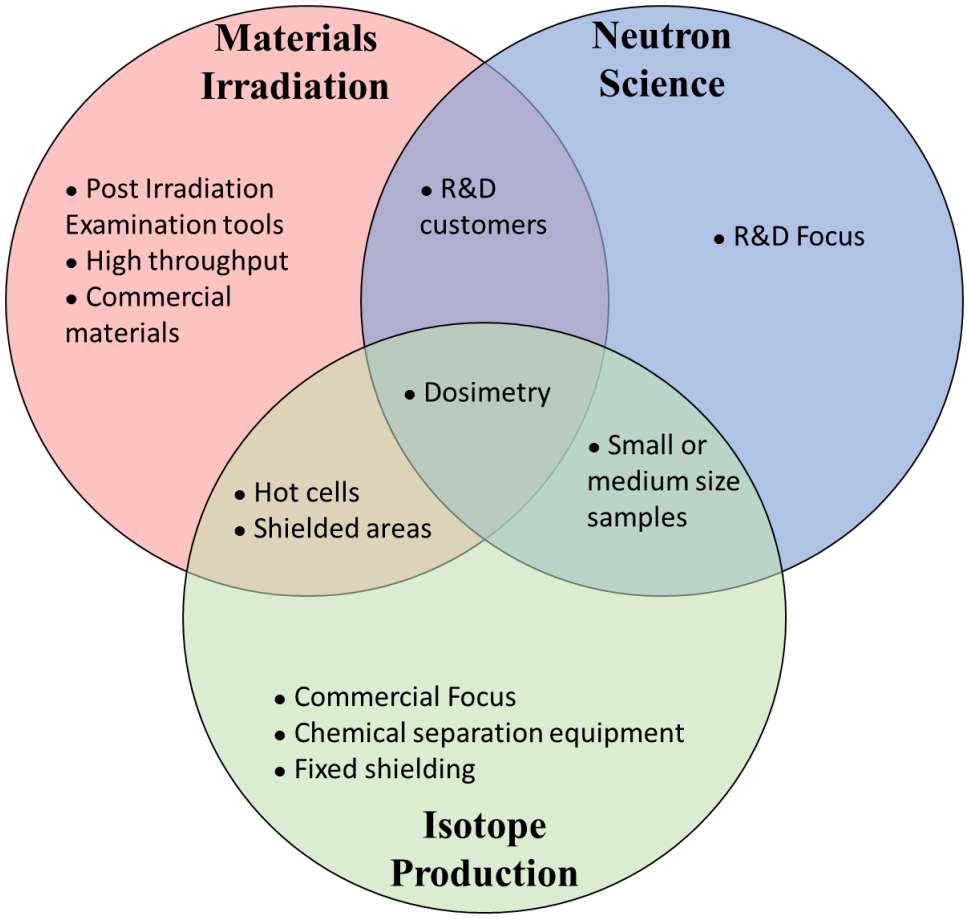

Figure 2-1: Commonalities between AUX facilities.

3. Material Irradiation and Testing Facilities (MIFs)

3.1 Intro to MIF

MIFs support the equipment and process areas used to replicate high-level radiation conditions and study its effects on irradiated targets. MIF neutron irradiation positions for materials are differentiated by the desired conditions and neutron fluxes. Major targets or materials utilized in MIF testing are typically separated into 3 categories:

- Neutron Activation Analysis
- Test fuels for qualification
- R&D/Commercial materials (gems, silicon)

Neutron Activation Analysis (NAA) is a method that is used to determine trace elements based on the characteristic radiation given off from the radionuclei formed by neutron irradiation. NAA techniques comprise the majority of irradiation activities in research reactors. NAA uses thermal neutrons due to the large cross-section most elements have compared to epithermal or fast neutrons. The larger thermal neutron cross-section is why most RR have positions within the reactor that have been optimized for thermal neutron output. Fast and epithermal neutron positions exist however in RR that can accommodate the extra neutron irradiation positions, and NAA with epithermal or fast neutrons can have the advantage of targeting specific radionuclide formation due to their smaller cross-sections, especially for elements that have very high thermal cross-sections. [1] [2]

Test fuels from the second category are put in an irradiated environment to reproduce reactor conditions after which post irradiation examination tests are performed to qualify the material for use in a reactor design. Silicon and gemstones may be irradiated for research and development and to produce commercial materials for use in integrated circuits and other consumer products. These materials are bombarded with neutrons to change the chemical structure of the material or dope the material with trace quantities of activation products. This work does not generally produce long-lived radioactive isotopes and no chemical separation is performed. Due to the commercial benefit from having a MIF with a research reactor, these facilities are found at most university RR that can support irradiation of materials within the reactor.

While isotope production is out of the scope of this report, research reactors that perform isotope production carried out by irradiation of targets typically requires a specific setup of hot cells and chemical separation equipment that will additionally alter the footprint of a facility. Due to this, medical isotope production facilities have different requirements that set them apart from MIF. Primarily, the hot cell configuration in a medical isotope production facility will focus on chemistry equipment capable of separating isotopes produced in a reactor target material in hot cells. After separation has been completed, the collected medical isotopes must be packaged and decontaminated while in a hot cell or glove box environment. Additionally, the chemical waste produced from the separation process must either be reused (requiring additional extractions) or disposed of. Finally, a medical isotope production facility requires general chemical laboratories to test the medical isotopes for quality and purity on a regular basis. Further discussion on medical and industrial isotope AUX facilities can be found in PRO-X-2022-008. [3]

3.2 Typical Attributes of MIFs

Neutron irradiation positions and support systems in MIFs differ based on several factors:

- mass and volume of sample
- the energy of the neutrons (fast, epithermal, or thermal)
- desired neutron flux
- volume and mass of sample to be irradiated
- time required for irradiation, and
- irradiation environment

These factors will influence the neutron irradiation positions and transport systems used in a RR. Shown below is an example of the many neutron irradiation positions available to a RR.

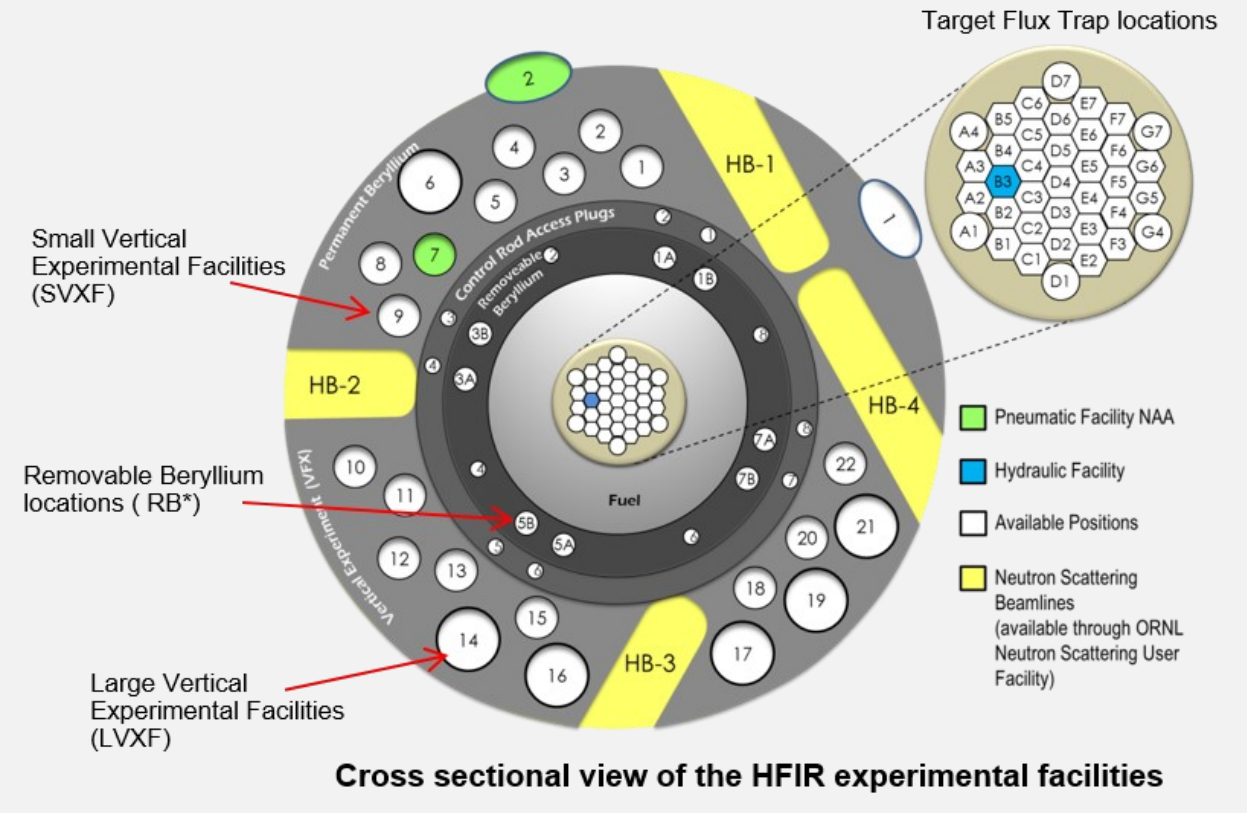

Figure 3-1: Example view of a RR (ORNL HFIR) with mark outs for materials irradiation research. [4]

As shown in Figure 3-1, a research reactor can have many different neutron irradiation positions that use different systems to deliver samples to an intended irradiation position. These include pneumatic and hydraulic systems for larger and smaller samples, vertical irradiation positions for inserting large samples mechanically, and beamlines that can be used by neutron optics experiments or stationary materials irradiation experiments.

3.2.1 Power, Run-Time, and Throughput

Reactor power and runtime for MIFs is varied based on the types of irradiation positions and projects being carried out at the facility. University RR power output is typically recorded in steady state between 1–6 MW. A high neutron flux is desirable, and RR are typically designed with reflectors to maximize this number. Most surveyed RR can produce neutron flux ranges of 1E12–1E13 neutrons/cm^2/sec. Flux in this range is considered typical for reactors that perform Si doping. [5] The typical neutron flux in low power level reactors varies from 2.5–10E11 n cm^{-2} s^{-1}, while the flux range is between 0.1–10E13 n cm^{-2} s^{-1} for medium-to-high power reactors, meaning most surveyed reactors fall in the medium to high range. This is because materials being irradiated act as neutron absorbers, so the reactor cannot be a low power to accommodate a loss of neutrons by irradiated materials without shutting down. A collection of power and max thermal flux reported by surveyed RR in the U.S. can be found in

Table 3-1.

Table 3-1:Survey of RR power and thermal neutron flux.

University	RR site	Power (MW)	Max Fast Flux (n cm^{-2} s^{-1})	Max Thermal Flux (n cm^{-2} s^{-1})
MIT	MITR-2	6	1.2E14	3.6E13

Penn. State University	PSBR	1.1	1.7E10	3.3E13
Missouri University of Science	MSTR	0.2	2.65E12	2E12
Idaho state	ISUR	5	-	3.8E8
U. of Madison Wisconsin	UWNR	1	3E13	3.2E13

3.2.2 Materials Handled and Throughput

Older RR use high enriched uranium fuel but there has been a concerted effort to convert these reactors to use low enriched uranium fuel due to proliferation concerns. The amount of nuclear material usable by a research reactor is heavily regulated by the NRC Rules of General Applicability to Domestic Licensing of Byproduct Material. [6, 7]

3.3 Neutron Irradiation Systems in MIFs

3.3.1 Capsule Systems

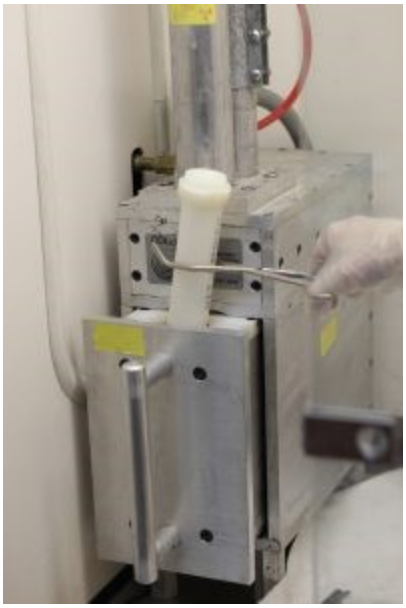

Figure 3-2: Rabbit tube sample capsule (UWNR)

Capsulized pneumatic or hydraulic systems (Figure 3-2, above) are a series of tubes that penetrate the moderation tank of reactor. Depending on the method of propelling the sample into the moderation tank, the system might be known as a rabbit tube (for pneumatics) or whale tube (for hydraulics). The tubes are made from metals such as titanium or polymers such as polyethylene. Samples are encapsulated in a shell (polymer or metal) and driven by pneumatics or hydraulics to transfer the encapsulated sample directly into the grid of a reactor core and remove it after some time. Due to the use of pneumatics or hydraulics, materials inserted into the irradiation capsule are limited in volume or mass. NAA is performed using this system, as the pneumatics/hydraulics allow for the samples to be inserted and removed from the reactor

quickly to measure short lived radionuclides. Similarly, smaller samples can be fed into control rods thus giving a high neutron flux of mostly fast neutrons. Control rod positioned samples can only be changed out when the control rod is not in the reactor and is thus limited in exposure time lengths. Gases used for the pneumatics are inert, such as CO_2 or N_2. Neutron flux provided can be as high as the unmoderated neutron flux produced by the reactor due to the placement of the system.

Ideal neutron flux for NAA and pneumatic tubes is around 5E11 n cm^{-2} s^{-1} for most elemental analysis. This allows for most elemental radionuclides to be measured. The short-lived radionuclides may be measured with lower flux, but longer-lived radionuclides require a higher flux or restrictively long irradiation times to be measurable. For NAA performed using epithermal or fast neutrons, pneumatic sites will have specialized shielding either on the capsule or on the pneumatic system to prevent thermal neutrons from penetrating while allowing epithermal or fast neutrons to irradiate the sample. For cyclical NAA, a recycling system for the sample is required. Though the footprint of the pneumatic or hydraulic sampling system itself is relatively small, shielding is required in the pneumatic system to prevent unwanted exposure to radiation that might damage or alter the sample during its travel to and from the irradiation position. Additionally, a variety of support equipment for the analysis of irradiated materials is required. Storage space for irradiated samples must be shielded to minimize external dose. Table 3-2 below shows typical sizes for pneumatic tubes at research reactors, maximum thermal flux, and irradiation time as well as the material the tube is made from as reported.

Table 3-2: Example rabbit tubes and associated parameters of surveyed RR.

RR site	Tube diameter	Total mass or volume	Thermal Neutron flux (n cm^{-2} s^{-1})	Tube time	Material
MITR-2	1 inch (1PH1) 2 inches (2PH1)		8E12 5E13	10 s – 10 min > 10 hrs.	Polyethylene Titanium
PSBR	N/A		1–3E13	10s -10 hrs.	N/A
MSTR	2.22 cm	16.9 g	4.36E12	No longer than 9 hrs.	
ISUR	1.59 cm				Polyethylene
UWNR	1.25 inches		4E12		Polyethylene

3.3.2 Mechanical Systems

Figure 3-3: Water test loop (silver tube) and crane (orange) shown with guide shown (MITR).

For larger and heavier samples that and be lowered into grid positions, mechanical systems are used. These systems typically have baskets that are loaded with material to be irradiated and are raised and lowered into position while attached to a cable line. This mechanical system can also be a crane or similar that can reach the reactors core (Figure 3-3). While larger samples utilize this method the exposure time tends to be shorter. Geochemical studies and geochronology use mechanical irradiation systems, with the USGS TRIGA reactor (Denver, CO) operates using a manually lowered small sample into a TRIGA tube using that is placed into irradiation position with a lazy Susan or central thimble depending on desired neutron flux/temperature. This system is simpler and cheaper than using cranes for placing samples into desired irradiation positions.

For an example of a mechanical system, MITR has a polar crane system that is capable of inserting samples into the core. This crane uses both 20 and 3-ton hooks. In addition, this crane is used for hot cell maintenance and movement and attaches to the concrete plugs located in the roof of the cells.

3.3.3 Test Loops

Figure 3-4: The Naval Reactor test loop at the Advanced Test Reactor (ATR) at Idaho National Laboratory (INL).

RRs that have medium to high power utilize closed test loops to prototype novel fuel elements for commercial power reactors or other reactor configurations (Figure 3-4). Loops are similar to hydraulic tubes but push fuel samples through forced coolant tracks to replicate reactor conditions. These loops have a much larger throughput than rabbit tubes and can have portions of the loop in different proximities to the core of the reactor to obtain a variety of environments. A test loop is designed to isolate the test fuel sample from the rest of the reactor to provide a controlled environment. Due to the complexity of test loop techniques, however, most test loops are at government owned RR (national laboratories) or the largest university programs. [8]

Higher thermal and fast neutron flux in the order of 5E15 n cm^{-2} s^{-1} is used to reach complete fuel burnup in a test loop sample, though lower flux of 1E14 n cm^{-2} s^{-1} can be used. Test loops occupy space in the reflector region close to the core of the reactor and require several pieces of equipment to monitor and control the temperature of the sample, equipment to monitor fission product production in the test loop coolant, fluence monitoring on the sample, fuel performance monitoring equipment and shielded cooling facilities for the sample after it has been run in the test loop. Additionally, equipment to monitor in-loop loss of coolant or similar accidental testing incidents is important, as are capabilities to ramp the power of the reactor and cycle the reactor. Footprints of test loops external to the reactor are noted to take up 5–25 m^2 of floor space.

3.3.4 Commercial Materials Irradiation Systems

Many of the attributes that make a MIF useful to a RR also make it useful to materials irradiation for commercial purposes. A major commercial material processed in MIFs is silicon in a process known as neutron transmutation doping (NTD). NTD as an income generator is a compelling case for many MIFs to include NTD facilities. Demand for NTD silicon is rising with the expected demand of 1000 tons of NTD Si estimated for 2030 to meet demands of new technologies. Larger dedicated NTD facilities should be able

to produce 20–30 tons of NTD Si per year, and as reactors reach the end of their lifespan and new reactors are built, an optimized dedicated irradiation position and system for NTD Si production might start with more simple irradiation rigs with expansion capacity only required if a reasonable expectation of the increase in demand for the NTD Si produced from the reactor, rather than building more specialized and custom made systems for NTD of Si. [9]

The NTD process is achieved by activating the Si-30 isotope into stable P-31 which gives a homogeneous distribution of the doping in the silicon. This process requires a very regular flux of neutrons with the power and size requirements based on initial resistivity of the silicon, desired resistivity of the silicon, and the total neutron flux of the RR. NTD of Si is usually performed using open beam ports that reach all the way through a reactor or by lowering pneumatic capsules containing the silicon into positions in the reactor pool.

Lower power RRs (250 kW) with neutron flux in 1E12 n cm^{-2} s^{-1} are capable of performing NTD on smaller but still usable quantities of Si. RRs that are more dedicated to commercial production can handle greater quantities of Si, but the thermal neutron flux must be greater than 1E13–1E14 n cm^{-2} s^{-1} to achieve the typically desired upper limit of 1000 Ω/cm resistivity. A Si ingot is typically a cylinder with a diameter between 5 and 15 cm and up to 70 cm of length, larger sizes being more common.

Irradiation of Si in a beam tube that is horizontal to the RR may not induce ideal thermal neutron activation, but the inclusion of shaped neutron shielding can achieve a homogeneous flux throughout the entire irradiation system which would increase the size requirement of this system. Other techniques such as rotating the ingot (which is used at MITR and OPAL) as it travels through the beam tube requires specific equipment that can make these adjustments to the position of the ingot and would also increase the footprint of the system. A good example of a dedicated NTD system can be found at MITR, shown in Figure 3-5 below.

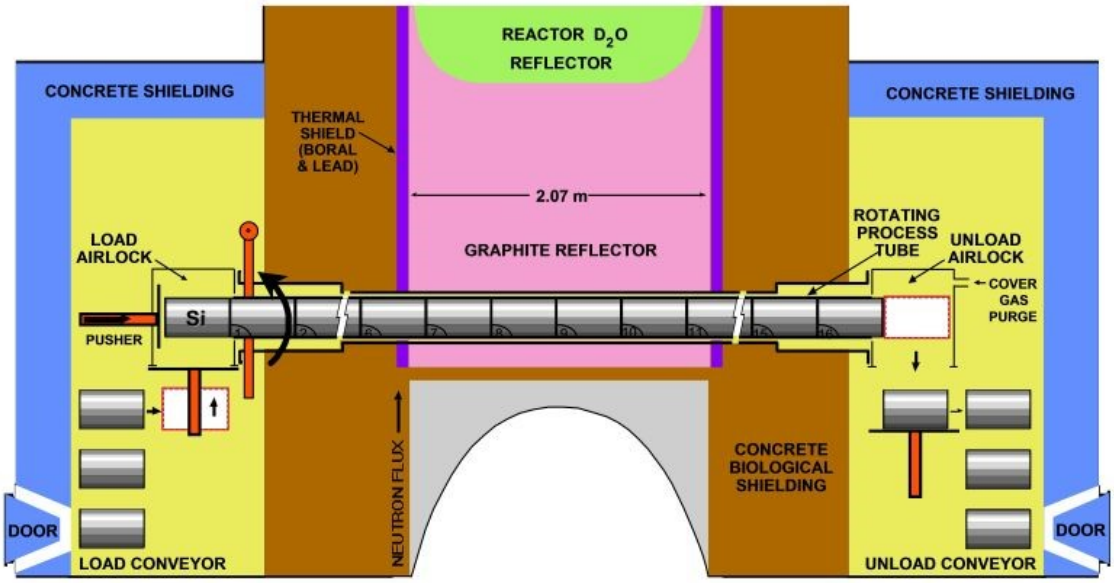

Figure 3-5: An example schematic of the silicon doping process at MITR. [4]

Gemstone transmutation is another commercial irradiation technique. Irradiation of gemstones is performed to change the crystal structure of the gemstone to acquire a specific desirable color of the gemstone, which increases their commercial demand and value. The most common gemstone this technique is used with is

topaz, which undergoes regular color changes from orange to blue with increasing exposure time, however diamonds or other gemstones may also undergo radiation treatment to induce color changes.

Gemstones are typically batch irradiated in containers that can handle around 2 kg of stones. For gemstone irradiation, fast neutrons are the most desirable, so the containers used for the irradiation process are covered with thermal neutron shielding. The temperature during irradiation must be controlled, so the containers must have their own thermal regulation equipment or some other method of cooling the stones during the irradiation process. Desirable temperatures for irradiation are between 100–150 °C, and temperatures that rise above 300 °C can cause discoloration or flaking of the gemstone. Heat load can be removed using coolant, but if water is used the fast neutrons irradiating the stones will shift to thermal neutrons, causing issues with the overall irradiation process.

Equipment required for gemstone irradiation includes the irradiation container which is covered in cadmium or boron shielding to shield against thermal neutrons. Coolant can be small amounts of water that is flowed through the container or an inert gas (such as nitrogen or argon). Inert gas as a coolant will increase the cost of the process, however. The irradiation chamber can be placed in an aluminum clad tubing if in a grid position, or a beam tube in a similar position.

Due to the competitive nature of these commercial techniques, details on gemstone irradiation are typically kept secret by the commercial entity performing the irradiation. This is further complicated by the constantly shifting nature of the gemstone market that is heavily dependent on cultural influences for determination of which gemstone sizes or coloring are currently in demand. Due to the constantly shifting nature of the gemstone market, and the nature of typically strict scheduling and procurement of the original stones, irradiating the stones, and then allowing for decay of the stones after irradiation, many RRs may find gemstone irradiation a difficult endeavor to include in their schedules. While several RR are pursuing gemstone irradiation worldwide, only three U.S. RR have the applied for the license to irradiate gemstones. [5]

3.4 Hot Cells or Glove Boxes

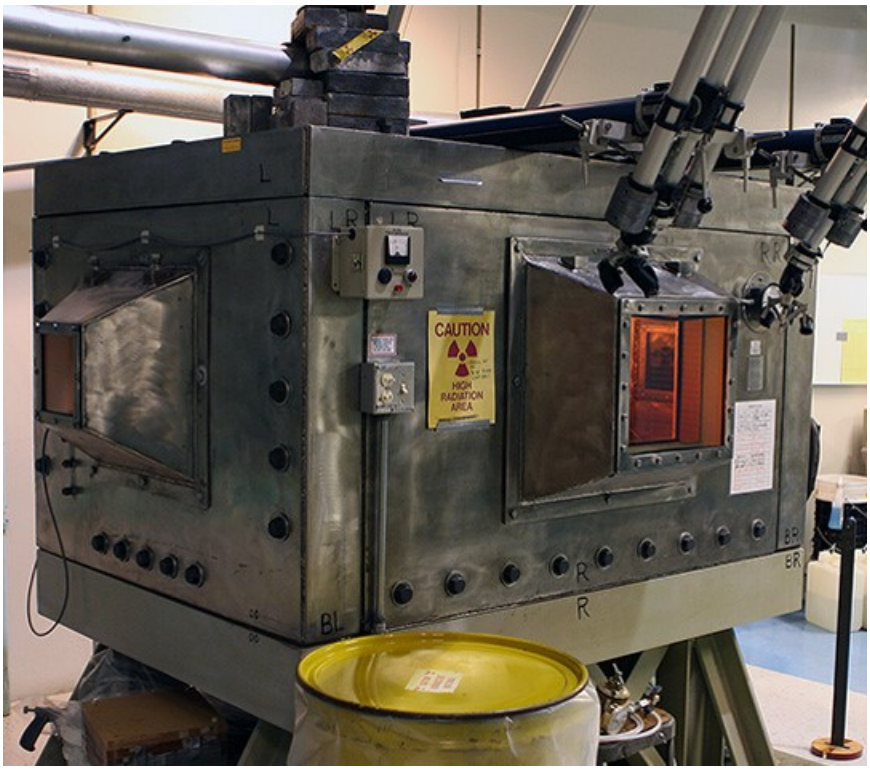

Figure 3-6: Example RR Hot cell with manipulators at MITR. [10]

Shielded radiation containment chambers, conventionally known as hot cells, are used to handle materials too radiologically active to be handled by a person wearing only personal protective equipment. They are a necessary tool for the conduction of materials research and PIE but are extremely expensive and require periodic maintenance. However, hot cells can also house equipment that can be used for extracting radioisotopes in isotope separation facilities, making them a large focus for PRO-X AUX proliferation reduction. Figure 3-6 above shows an example hot cell at MITR, which serves and inert-atmosphere box for handling molten salt test fuels. [11] In addition to shielded radiation cells, some work may be done in lower shielded glove boxes or fume hoods if the activity of the sample is low enough. For example, MITR has several fume hoods and an inert atmosphere glovebox with 4 ports and a furnace for handling materials outside of the reactor exclusion area. [4] [10]

Table 3-3 lists surveyed hot cells from various Department of Energy (DOE) facilities and their associated sizes. DOE hot cells were listed as the highest upper bounds of hot cell size and operational flexibility. Commercial and RR hot cells will be smaller than the listed hot cells.

Table 3-3: Surveyed DOE research hot cell details.

Facility	# Of hot cells	Hot cell sizes
ANL/IML	4	6 ft x 5 ft x 9 ft 8 in (L x W x H)
INL/ARL	6	Not listed
INL/EML	N/A	Not listed, primarily related to capabilities for handling radiological samples
INL/IMCL	N/A	Not listed, primarily instruments contained in modular radiological shielding and confinement systems.
INL/HFEF	2	70 ft x 30 ft x 25 ft, 20 ft x 30 ft x 25 ft (L x W x H)

INL/FASB west-room	Not listed	Not listed. Stated to be a small set that houses an irradiation-assisted stress corrosion cracking system.
INL/FASB east-room	Not listed	Not listed. Like the west room, it also measures corrosion and crack propagation to help extend the life of light water reactors.
ORNL/IFEL or 3525	6	One is 10 ft x 24 ft x 14 ft, two are 10 ft x 35.5 ft x 14 ft, two are 64 in x 44 in x 44 in, one is 4 ft x 6 ft x 8 ft (D x W x H)
ORNL/IMET or 3025E	6	3 ft x 4.5 ft x 8 ft to 11 ft x 7 ft x 13 ft (D x W x H)
ORNL:/7920	10	7 ft x 7 ft x 8.5 ft (L x D x H), one 4 ft x 3 ft x 4 ft
ORNL/7930	7	Cell A: 8 ft x 20 ft x 24 ft B: 16 ft x 23 ft x 22.5 ft C: 20 ft x 33 ft x 24 ft D: 20 ft x 41 ft x 13 ft E: 20 ft x 17 ft x 30 ft F: 15 ft x 37 ft x 13 ft G: 20 ft x 17ft x 30 ft (L x D x H)
PNNL/RPL-HLRF	3	A: 15 ft x 7 ft - 8.5 ft x 15 ft B & C: 6 ft x 15 ft x 8.5 ft (W x D x H)
PNNL/RPL-SAL	6	All are 6 ft x 5.5 ft x 5.5 ft (L x D x W)
PNNL/RPL-modular	7	Three older units not listed. PDC1, PDC2 are 4.5 ft x 6.5 ft x 8.3 ft MEC1 6ft x 12 ft x 8.5 ft and MEC2 6 ft x 8 ft x 8.5 ft
SRNL	16	6 ft x 6 ft x 15 ft-18 ft (L x W x H)

3.4.1 Common Shielding and Support Systems

There are some common features that can be found between all hot cells, regardless of the purpose for which they are being used. Larger, immobile cells are usually shielded with at least 3 ft. of high-density concrete and lined with alpha-tight stainless steel to assist with decontamination. It is the size and thick shielding that make them ideal for examining spent fuel and highly irradiated materials. In contrast, smaller units are often shielded by stainless steel alone and can be moved with special cranes of forklifts. These are ideal for testing irradiated materials that aren't hot enough to warrant the extra layers. Additionally, cells are maintained at negative air pressures and outside air quality are maintained with advanced high efficiency air filtering systems and Venturi scrubbers at the facility in which they are installed.

On the other hand, hot cells intended for isotope production possess dedicated chemical facilities and separation systems such as dissolvers, and spectroscopic process monitoring, all things that wouldn't typically be found at a facility intended only to study irradiated materials. One such consideration is the atmosphere used inside of a hot cell; inert atmospheres are common in separations involving flammable solvents, such as hexone in the REDPX process. However, this would not be the only possible use of an inert gas. For example, Ar is used at fuel examination facilities because it is an excellent gas shield for welding and cutting. This is illustrated at INL's HFEF, where moisture and air levels are critically maintained below 60 ppm. Another distinguishing characteristic for a hot cell chemical separations facility would be the additional filtering systems involved, which include alkaline scrubbers and iodine retention platforms in the stacks. This report is not intended provide an exhaustive account of isotope facilities, so a further description of them will end here.

To remotely view the inside of a hot cell, cameras are often be used, though they must be periodically replaced. More often, thick, oil filled Pb windows are used for direct observation of the inside of a cell. The

oil usually provides optical coupling, though they sometimes serve as neutron absorbers. Another option for hot cell windows is to fill them with a zinc-bromide solution, which allows the glass to self-heal from radiation damage. However, differences in the refractive index often leads to image distortion, which can make material handling more difficult and the $ZnBr_2$ solution can often leak. Pb-vinyl or W-loaded gloves can be used for lower activity samples, though handling is more frequently carried out with remote master/slave manipulators.

3.4.2 Fuel Examination Facilities

The support systems surrounding a hot cell vary greatly depending upon the program the hot cell supports in a MIF. For example, a facility dedicated to examining or processing spent nuclear fuel and or fuel pins would possess the logistics for moving fuel rods and assemblies to very large cells. For larger samples the facility would include things like large bay doors for receiving shipments by truck or rail, large overhead cranes and hoists and pneumatic transfer stations. Casks are safely disassembled on site, with the help of multiple examination and testing techniques. PIE-focused facilities would host equipment to support mechanical, thermal, and imaging techniques that often overlaps with those found at a materials characterization facility such as gamma scanning, electron microscopes, DSC, and tensile testing. Often, use of these various testing techniques requires special preparation, e.g., metal, and ceramic powder processing, requiring equipment used for atomizing, milling, mixing, pressing/sintering, grinding, and polishing. Keeping the metallurgical equipment clean is also of the upmost importance, so decontamination cells are also necessary. These usually have turntables that spray water or steam onto contaminated equipment and supplies to clean them.

As a specific example of a hot cell found bank in a MIF, the primary cell bank at HFEF is 70 ft x 30 ft x 25 ft with 4 ft thick high density concrete walls and an inner surface lined with stainless steel. It's fitted with two 5-ton bridge cranes and 15 workstations, each with a 4ft thick window of oil filled Pb glass and a pair of remote master/slave Electro-mechanical manipulators rated for 750 lb. In addition to the decontamination cell, sleeves are used to cover casks when transferring them from the loading bay to the hot cell through a dedicated tunnel. The facilities here are numerous and thorough, making it quite unique. Its proximity to the NRAD reactor allows for the use of neutron radiography as an additional imaging technique. Additionally, furnaces in the hot cell can reach 2,000 °C for extended periods, something that is quite important for simulating accident conditions when testing new materials. Like HFEF, different labs will have different capabilities and limitations, which ultimately affects what kinds of fuel or other material can be received.

3.5 Post Irradiation Examination Techniques

One primary capability of a MIF is PIE activities. These focus on failure modes that occur during irradiation over normal use in a reactor, which can include swelling of the material, non-thermal deformation, cracking, and the production of fission off gassing. Many of these issues are linked to fuel performance and burn-up, affecting the amount of energy that can be extracted from nuclear fuel. To study these failure phenomena, both for commercial use and materials research, PIE involves several techniques that can be divided into destructive and non-destructive techniques. An overview of surveyed hot cell PIE equipment found in DOE facilities is shown in Table 3-4. Due to the flexibility of hot cells at many DOE facilities, they serve as a bounding condition for PIE techniques, as hot cells that are dedicated to a specific technique can be smaller and have more specific shielding requirements.

Table 3-4: Typical Hot cell set up and equipment for MIFs used in post irradiation examination.

Facility	Typical Hot cell Equipment
ANL/IML	Pb shielded gloveboxes • laser welding system • vacuum fusion device • Electric Discharge Wire Cutting Machine • SEM • TEM • macro-cameras • laser profilometer • contact micrometers • dial-gauge micrometers • servo hydraulic driven tension/compression/cyclic testing machine • Internal radiant furnace
INL/ARL	• Gloveboxes • fume hoods • Gas chromatograph • Gas pressurized extraction chromatography (GPEC), both manual and automatic • Counting labs (gamma, alpha spec, gas flow proportional counters liquid scintillation, low background counting lab in pre-WWII steel vault using low background concrete) • Mass spectrometers [portable gas, high resolution multi-collector fission gas (MC-GMS), Inductively coupled plasma (Quad-ICP-MS), Inductively coupled plasma time of flight (ICP-TOF), multi-collector inductively coupled plasma (MC-ICP-MS), thermal ionization (TIMS)] • Elemental analysis [Optical emission (ICP-OES), Femtosecond laser-induced breakdown spectrometer (fs-LIBS)] • Light element (CSONH) combustion and inert fusion analyzers • Capillary electrophoresis (CE) • High performance liquid chromatography (HPLC) • XRF • Microwave-assisted digestor • 3D laser scanning confocal microscope • 4K digital microscope • Hot cell particle picking microscope • Hot cell entrained gas collector • Mass separator (rad and non-rad) • Non-destructive barrel scanner • Hot uniaxial press (HUP), muffle, well, and tube furnaces • Glovebox advanced casting system (GACS) furnace • Wet chemistry labs
INL/EML	• JEOL JSM-7000f SEM with EDS, WDS and EBSD detectors • Gatan precision ion polishing systems (PIPS-2) • Gatan precision etching and coating system (PECS) • FIB/SEM workstation from TESCAN, equipped with Aztec Oxford Instruments suite for EDS/EBSD characterization, LEICA cryo-stage, and Alemnis nanomechanical testing. The microscope is equipped with an Omniprobe200 manipulator for in-situ sample lift out, and two gas injection systems for carbon and platinum deposition. • FEI Talos F200x S/TEM equipped with Super-X EDS, Gatan Quantum EELS and ASTAR/TOPSPIN systems
INL/IMCL	SSPA - Shielded sample preparation area with optical microscope, polishing and grinding, sample cutting in hot cell, glovebox, and hood • SEM - JEOL 7600 • EPMA – Shielded Camera SX100R • STEM – FEI Titan equipped with probe corrector, super-X EDS, EELS, DEN Solutions D6 heating holder (1573 K), tomography holders, vacuum transfer holder, Hysitron PI-95 Pico Indenter • APT-LEAP 5000 Atom Probe • Shielded FIB-FEI Quanta 3D FEG Focus Ion Beam • Shielded FIB-Thermo G3 Plasma Focus Ion Beam • FIB-Thermo G4 Helios Hydra Plasma Focus Ion Beam with TOF-SIMS, equipped with EDS and EBSD • shielded LFA-Netzsch LFA 427 laser flash analyzer • shielded TGA/MS – simultaneous TGA/DSC+MS Netzsch STA 409C Skimmer (RT-2000°C) • shielded Thermal Conductivity Microscope with spatial resolution of 50 µm from RT-300°C • Quantum Design PPMS equipped with electrical, thermal and magnetic properties from 1.8-400 K and 0-9 T • PANalytical powder XRD • Zeiss Xradia 520 Versa XRM for materials of length from 0.1-100 cm • shielded mini-tensile tester with digital image correlation
INL/HFEF	NRAD reactor • Autoradiography • Visual examination machine • Eddy current probe for measurement of oxide thickness • Precision gross and isotopic gamma spectrometer • Element contact profilometer bow & length machine (fuel rods) • Profilometry and eddy current measurement bench (fuel plates) • Pycnometer • Laser puncture gas collection and analysis system • Fuel accident condition simulator (FACS) furnace • Metal waste form furnace • Remote load frame
INL/FASB west-room	• Irradiation-assisted stress/corrosion cracking hot cells • Two inert fuel development gloveboxes • Pyrochemistry glovebox • Three radiological hoods and one non-radiological

	hood • Thermal properties characterization instruments (laser flash, dilatometer, DSC) • Cobalt-60 gamma irradiator • Lab-scale fabrication equipment (hot isostatic press, arc melting furnace) • Metal and ceramic powder processing equipment (atomizer, milling, mixing, pressing/sintering) • Numerous heat treating and sintering furnaces
INL/FASB east-room	•Two inert fuel fabrication gloveboxes, both with Arc-melting furnace with casting capability, Hydraulic press, Gram-scale atomizer, Hydriding/nitriding apparatus, Inert box welding station • Inert pyrochemistry glovebox with Molten salt electrorefiner, Oxide reduction furnace, Sodium distillation furnace, Fuel form casting, Multi-function furnace • Three radiological fume hoods• Irradiation assisted stress corrosion cracking system, includes a Decontamination station, In-cell imaging microscope, Pressurized water reactor testing rig, Boiling water reactor testing rig• Fabrication equipment including Hot isostatic press, Hot rolling mill, Multiple furnaces • Sample preparation and characterization, including High- and low-speed saws, Auto polisher, Three SEMs XRD, XRF, optical microscopes, particle-size analysis microhardness testing, Density measurement (helium pycnometer), DSC, Dilatometer, Laser-flash thermal diffusivity, Positron-annihilation spectroscopy, (Tensile, compression and bend testing), Ultrasonic testing • Cobalt-60 gamma irradiator • Solvent test loop
ORNL/IFEL or 3525	Largest three cells are main air atmosphere cells for handling NAC and T-2 casks or full-length LWR rod, 3 ft of high-density concrete shielding, stainless steel liners, oil-filled Pb windows. Fourth and fifth are stand-alone air atmosphere cells with 8 in steel shielding, respectively for irradiated microsphere gamma analysis and SEM. Last is also stand-alone air atmosphere for core conduction cool-down testing with 4 in Pb shielding. For metrology; metallographic separation by sectioning, grinding, and polishing of metal and ceramic samples; furnace oxidation, acid-base etching, decontamination, optical and electron microscopy; gamma spectrometry; and other physical and mechanical properties evaluations. Irradiated Microsphere Gamma Analyzer (IMGA) cell, SEM cell, decontamination activities, microscopy, photography of samples, and fracture testing of prepared specimens.
ORNL/IMETF or 3025E	All have concrete and steel shielding with air atmosphere, floor, and walls of one is covered with stainless steel. Restricted to beta/gamma sources. Tools for materials property tests (tensile, impact, hardness, compression, bending, fracture, toughness, crack growth) with different temperature and pressure environments. Profilometry and various forms electron microscopy. However, cells are flexible depending on installed/needed equipment. • SEM (PhilipsXL30) • Sample sorting and identification • Sample machining using a CNC milling machine and diamond saws • Furnace annealing • Automated welding • Ultrasonic cleaning • High-temperature, high-vacuum testing • Tensile testing with high-vacuum chamber option • Impact testing, fatigue, and fracture toughness testing of standard and subsize impact specimens • Automated micro-hardness testing • Profilometry • Laboratory Hood • Gloveboxes
ORNL/LAMBDA	The LAMDA is facility is multipurpose, covering approximately 2,500 ft^2 over three radiological laboratories. Unique in allowing for examination of low-activation materials without the need for remote manipulation, facilitating the examination of delicate samples that is not possible in traditional hot cells. Three multipurpose radiological labs in LAMDA provide containment and shielding adequate for evaluation with low radiological threat materials. Generally, radiological hazards are first screened and verified to have beta/gamma activity with a dose less than 60 mR/h at 1 ft. Samples with low-level alpha contamination are acceptable, though considered nonroutine and handled on a case-by-case basis. Research encompasses basic science, applied engineering, and regulatory work. Most common conducted jobs include mechanical testing, optical and scanning electron microscopy, densitometry, metallography, and finally thermal and electrical conductivity. Low pressure (vacuum to 10-7 torr) and high temperature (to 1300°C) testing is routine.

ORNL:/7920	The smaller cell is for decontamination, while one of the larger ones is dedicated to analytical chemistry instrumentation. Surrounding facilities includes analytical laboratories. Once per year, these hot cells are used to fabricate and process Pu, Am, and Cm from HFIR, as well as separate actinides such as Cf. Windows made of Pb glass and mineral oil. Pneumatic motor-driven intercell conveyor system. Fiberoptic access for online spectroscopic monitoring. Alpha and neutron emitter focus, hot and cold labs, high bay space.
ORNL/7930	Shielding a combination of steel liners and high-density concrete, windows made with Pb glass and $ZnBr_2$. Nearby 22 ft deep storage pool. Pneumatic transfer tube system. Fiberoptic access for online spectroscopic monitoring. Alpha and neutron emitter focus, hot and cold labs, high bay space.
PNNL/RPL-HLRF	30 T crane for receiving full length fuel rods, high density 4 ft thick concrete, oil filled high-density Pb windows. Oil is for optical clarity, no shielding function. All cells interconnected, Manual fire suppression and heat detection in ventilation ducts. Large hooks for moving casks and rods.
PNNL/RPL-SAL	Shielded with high density concrete and Fe.
PNNL/RPL-modular	Shielding for all cells is 12 in thick steel, and exhausts to main exhaust system. New hot cells in basement of the facility, will have Pb-glass windows. The hot cells will also have a manually actuated, dry chemical, engineered, fixed extinguishing system with fixed nozzles
PNNL/common	Radiochemical separations, tritium processing, analytical chemistry, nuclear forensics, PIE. Some techniques include • 7.05 T magnet with NQR spectrometer • gamma scanning • high resolution cameras • hydrogen isotope assay • ^{3}He of steel • surface analysis (XPS, Auger electron spectroscopy, SIMS) • thin film thickness measurements • gas and liquid extractions • elemental analysis • DSC • TGA • mass spectrometry • XRD • 8801 servohydraulic multipurpose testing system (tensile, compression and burst testing of high burnup cladding, static fracture, high and low cycle fatigue, and creep-fatigue testing, all up to 1100 °C in inert atmosphere) • FEI Helios 660 SEM • FIB and probe corrected JEOL CEM ARM300CF STEM with G2 camera, dual Bruker EDS detectors • FEI Quanta 250 FEG, equipped with EDAX, EDS, WDS, EBSD • high performance optical microscopes • polishing equipment
SRNL	3 feet high density reinforced concrete, cell wall lining of concrete and steel. Each air cell has one viewing window and two manipulators. Two 10-ton cranes, one above the cells and another in the truck bay. Cells have removable overhead covers, and some have cell-size rear doors at ground level, in addition to 11 X 11-inch chute doors for movement of smaller samples. Capabilities exist for the examination of fuel and full-length commercial fuel pins (visual and photographic examination, metallography, profilometry, eddy current, gamma scan). These can be segmented, and metal samples measured. Mechanical testing samples can be extracted for bend, compression, impact, or tensile testing. Specimens can be removed for examination in contaminated SEM or optical microscopy. There is also the capability to collect and measure fission gases. Physical, chemical, and radioactivity assessments and examinations can be performed, as needed.

3.5.1 Non-Destructive Techniques

Visual Inspection

Visual inspection and photography are used to observe macroscopic changes on surface of a fuel element. It is important for detecting material failures stemming from effects such as corrosion and its product

deposition, cracks, and swelling due to manufacturing and/or radiation conditions. Periscopes with built-in magnification and specialized cameras are typical for this kind of work. Visual inspection is carried out in hot cells or the pools where spent fuel is stored.

Profilometry

Profilometry refers to the measurement of the surface profile by either optical or mechanical (surface) means. More specifically, inspectors are typically interested in making regular measurements of the diameter along a fuel rod at regular, mm scale. This allows for the detection of bow defects and ovality of cylindrical fuel elements. Xe migration has even been studied with when combined with secondary-ion mass spectroscopy (SIMS). [12] Accuracy is maintained by linearization of transducer elements in the profilometer. Contact profilometers are more common at fuel examination facilities, while optical variations can be found at materials characterization facilities.

Eddy Current Testing

Eddy current testing is a very sensitive method for providing information on the integrity of irradiated fuel cladding. It is primarily a surface technique, which depending upon measurement parameters can reach material depths on a mm scale. The test probe consists of a coiled Cu wire with an applied AC current that produces an oscillating magnetic field in the vicinity of the coil. This in turn produces eddy currents along the surface of the conducting fuel rod according to Lenz's law, which are affected by surface abnormalities defects such as longitudinal and circumferential notches, holes, and other discontinuities.

α Autoradiography

Alpha autoradiography measures alpha particles produced by a material's natural radioactive decay processes. Images are often produced on an α-sensitive film (e.g., cellulose nitrate) or phosphor screen, with chemical processing often being necessary for the films. Due to the inherently weak penetration of α particles and energetic overlap of multiple emitters (e.g., ^{238}Pu and ^{241}Am) and more elaborate sample preparation, pure α autoradiography has been shown to be of limited use for irradiated samples, being practical only if β particles can simultaneously be counted on a finely polished surface. [13] [14] However, this method has shown great promise for determining high concentration regions of alpha-emitting Pu and U isotopes in MOX fuels, with increases in sensitivity being achieved by using UV-Vis and photoluminescence spectrophotometry on a CR-39 polymer radiograph. [15, 16, 17, 18, 19, 20] This is particularly important for quality control, as heavy-metal diffusion during the sintering process often leads to the formation of agglomerates in fuel pellets. This can lead to hotspots during irradiation, ultimately leading to a smaller burnup potential. [21]

γ Scanning

Passive Gamma Emission Scanning Tomography (PGET) is a swift way to characterize to characterize fuel rods without dismantling the fuel. Measurements are typically made on gamma rays that are the product of fuel decay. The flux intensity of this rod-penetrating radiation is measured multiple times at different orientations with a collimated detector, which allows images to be constructed with tomographic algorithms. When combined with a spectroscopic detection system, one can select for particular isotopes, which significantly expands the amount of information one can collect. This includes but is not limited to the axial and radial distribution of the fission products (FPs) in a fuel element, the migration of volatile FPs, initial ^{235}U enrichment, burn-up, cooling time and the geometrical characteristics of the fuel column.

Isotopes such as ^{154}Eu and ^{137}Cs are more commonly measured in this technique, because (1) They have ideal half-lives for measurement of most fuel elements (2) Possess well-separated energy states and (3) The

released gamma rays have energies capable of penetrating a dense fuel assembly. Common elements of the instrument include a collimator and high-purity Ge system with Compton suppression to filter background gamma signals that would overwhelm the low intensity gamma lines. PGET has also been applied interactively, such that transmission measurements from an active source are combined with the passive measurements. This allowed for the determination of material density as a function of burnup, and perhaps more significantly, a 3D reconstruction of the internal radial distributions of ^{134}Cs, ^{137}Cs and ^{154}Eu. [22]

SEM

In scanning electron microscopy (SEM), a focused electron beam is directed onto the sample surface and scanned in a raster pattern. The high-energy (15-20 keV) electrons interact with the surface in various ways, producing secondary electrons (SEs), back-scattered electrons (BSE), characteristic X-rays, cathodoluminescence and even transmission for thin specimens, as seen in scanning transmission electron microscopy (STEM). SE detectors are standard for SEMs, with BSE detection being especially complementary for the examination of nuclear fuel. Sample preparation is simple since samples are only required to be conductive, but the difficulty can be increased depending upon the degree/type of radioactivity. Specialized shielding and may also be necessary to protect the sensitive detector. However, the information provided by SEM is well worth the effort for studying irradiated materials.

Low energy, inelastic SE are responsible for producing surface images of a sample surface, allowing for the observation of morphology changes of materials upon irradiation. Because of the fundamentally small de Broglie wavelength of the scattered electrons, one can make finer microstructure observations than could be observed with optical methods. Higher energy, elastic BSE scatter much more readily with heavier, electron dense atoms, making the technique highly sensitive to the atomic number. Additionally, they interact at a greater depth than SE, allowing one to distinguish between different phases and compositions of a material within an imaged spot. One of many applications could be to examine the evolution of grain boundaries and deformations at various stages in the fuel cycle. [23] [24]

EBSD

Worth mentioning is electron backscatter diffraction (EBSD), which provides additional software and hardware not found in conventional BSE detection that provide only image contrast. In this technique, a flat polished specimen is tilted away from an overhead SEM electron beam and towards a phosphor screen and charge-coupled device camera. The BSEs diffract through the sample according to Bragg's Law and form Kikuchi patterns, which are essentially projections of lattice geometry planes, yielding direct information on the local crystalline structure and grain orientation near the surface. Since these patterns vary according to the base material and how it is prepared, a supporting database can be used to identify known phases in a polycrystalline aggregate. This kind of localized detail on textures and grain boundaries on polished metal surfaces can be quite difficult to obtain in traditional XRD and TEM, which are often better suited for powdered and ultrathin (nm) samples, respectively. [25]

It has long been known that grain size greatly influences fission gas release and swelling in composite fuel pellets, making its control highly important when characterizing nuclear fuel. EBSD thus provides a natural solution as both a quantitative and visual tool to quickly map grain boundaries. Similarly, orientation maps from this technique can also be used to understand the porosity, microstructure, and grain orientation, information that can be used to understanding material stresses and its relationship to gas release. [26] However, great care must be taken for sample preparation when applying EBSD to nuclear specimens in order to properly interpret and optimize results. [27]

X-ray spectroscopy (EDS/WDS)

Obtaining quantitative information from the distribution of elements in an SEM image requires the measurement of the characteristic X-rays. This is usually done via two methods, either with electron dispersive spectroscopy (EDS) or wavelength dispersive spectroscopy (WDS). In EDS, the energy of each X-ray is converted into a proportional voltage by a semiconducting solid-state detector. This process is mediated by a field-effect transistor component. In contrast, WDS separates X-ray signals based on wavelength, more specifically through the process of diffraction. This is done with a reference crystal, which only allows X-rays of a particular wavelength to diffract depending upon its orientation and lattice spacing. Practically, SEM/EDS/WDS measurements can provide data on element distribution with a surface depth and lateral resolution of about of 1.0 µm.

There are some important practical differences between EDS and WDS. EDS, which is more commonly found in commercial SEMs, is a much faster techniques since it simultaneously counts all the X-rays with electronic detection, but this comes at the cost of low reproducibility and count rates. Regardless, because of its ease of use with most commercial SEMs, this method is more ubiquitous for the elemental analysis of spent fuels. [28, 29] On the other hand, WDS is a much slower mechanical technique, since it relies on mechanically manipulating a crystal to measure characteristic X-rays for one element at a time. But this comes with the advantage of much higher resolution and lower detection limit, which can be useful for which can be useful for lighter elements like O (MOX fuels), B (B_4C fuel coating) and C (e.g., B_4C and ZrC neutron absorbing fuel coatings). [30, 31, 32]

EPMA/EMPA

At its core, electron probe microanalysis (EPMA), or electron microprobe analysis (EMPA) is the combination of electron microscopy and X-ray spectroscopy, usually WDS. In this technique, electrons with an energy on par with SEM are beamed towards a sample, causing it to emit X-rays that are characteristic to the element(s) being examined. [33] As expected, this technique can be used as an SEM. However, what makes this particularly useful is its ability to simultaneously determine element concentration and distribution, with a lateral resolution of up to approximately 0.5 µm when coupled with the WDS. In practice, EPMA is used to methodically identify phases in irradiated fuel, which can consist of (Xe, Kr and I, Cs) or non-volatile (Sr, Ba, Y, Zr) fission products, in addition to additives or other actinides. [34]

µXRD

Micro X-ray diffraction (µXRD) allows for structural examinations of nuclear materials at the lattice scale. Unlike conventional XRD which emits a beam with a diameter at least a few hundred micrometers, µXRD uses specialized polycapillary X-ray optics to focus a divergent X-ray source to a diameter tens of µm wide. This results in a much higher spatial resolution, which allows one to spot details that would otherwise be averaged out over a larger surface area. For example, µXRD has been shown to reveal diffraction spot stretching along the azimuthal direction, also known as azimuthal reflex streaking. This is caused by crystal deformations and is usually accompanied by dislocations and sub-grain formation. These defects are practically observed by variations in the number and intensity of diffraction peaks, which in turn depends on the size and orientation of grains. [35] This technique has been applied to a variety of nuclear fuels. For example, it has been applied to Pu-U mixed oxide fuel pellets to obtain grain size and distribution changes after irradiation. It has also been used to observe lattice changes with regards to high-burnup UO_2. [36, 37]

μXRF

Micro X-ray Fluorescence (μXRF) is yet another X-ray technique, particularly for accurate elemental analysis. It is like SEM in that characteristic X-rays are generated from the sample, with the key difference being that the excitation source is a very narrow X-ray or gamma ray beam, similar in size to what is found in μXRD. As before, EDS or WDS is used to quantify and map the elemental composition/concentration in fuel, usually with detection limits of 100 ppm and a lateral resolution around 1 μm. This technique has shown a great number of advantages for elemental spatial resolution in Pu and mixed-oxide applications. [38] However, despite its usefulness, this method is disadvantageous in that this sample preparation and analysis often require great effort, and beamlines often have activity exposure limits. [39]

μXAFS

Fundamentally, X-ray Absorption Spectroscopy (XAS) measures an X-ray absorption coefficient as a function of the applied energy when it is at or equal to the binding energy of core electrons. These absorption events result scattered photoelectrons, which are modeled and interpreted according to the absorption region. In extended X-ray Absorption Fine Structure (XAFS), the energy of the photoelectron is so great that the scattering cross section of neighboring atoms is weak. Because of the different electron binding energies of various elements, μXAFS is a very element specific technique, and has been used to characterize the atomic environment of many actinides, providing a wealth of information that XRD cannot. This includes average distances to neighboring atoms, average distances, and oxidation state. This information can be used to understand speciation of nuclear fuel, which can greatly assist in non-proliferation efforts. [40]

Neutron Radiography

Neutron imaging is based on the attenuation, through both scattering and absorption, of a directional neutron beam through matter. Given that different materials vary in their ability to attenuate neutrons, then both composition and structural information can be obtained in ways that are complementary to X-ray techniques. Neutron beams must be generated in a reactor from a neutron emitting isotope or a target in a proton accelerator before being focused into a specialized beamline, somewhat limiting the prevalence and accessibility of this technique.

Regardless, neutron radiography is a versatile in that it can provide data on the condition of nuclear fuel such as fuel swelling, void formation, burn-up and enrichment variations, pellet-clad interactions, pellet-clad and pellet-pellet gaps, pellet cracking, and material migration on materials. This is possible on even on high-gamma emitters, which can interfere with conventional X-ray imaging techniques. Many variations are available, and the proper choice depends upon the application and desired results. Neutrons don't directly produce an image but do so indirectly through radiation emitted as a result of their use. The secondary radiation can either be monitored by digital detectors or recorded on photographic/cellulose nitrate film, activation foils, or photostimulable storage phosphor plates.

One great advantage/complementary feature of using neutrons in radiography is their ability to pass through tens of mm of commonly used engineering materials such as Al and steel. This is in opposition to X and gamma rays that are both absorbed and scattered by electrons. This makes higher Z elements more sensitive to atomic weight with respect to absorption; however, neutrons possess no such Z trend since they instead interact with nuclei and often in no apparent pattern. For example, neutrons are absorbed by both Cd and H, despite their large difference in atomic weight. The ability to detect hydrogen is especially important, especially for the dense Zr alloy cylinders used in fuel rods, as they often absorb hydrogen from

an oxidation reaction with water. This hydride effect can result in embrittlement but can be studied in detail with neutron radiography. [41]

Laser Flash Analysis

Since it was first introduced, the laser flash method has proven to be a very fast, reliable and non-destructive way of measuring thermal properties such as thermal diffusivity and heat capacity for small samples small as 6- 12 mm in diameter. [42] The method works by exposing the material to a powerful laser pulse, which briefly increases the temperature at the front surface of exposure and creates a thermal gradient. As the heat diffuses to the back of the sample, the heat flow is measured as a function of time until equilibrium is reached. A standard model formula for determining thermal diffusivity was determined by Parker, et al., though care must be applied when applying it to irradiated materials, as crystalline defects for radiological materials are not necessarily in equilibrium under rapidly changing conditions. [43] Such changes can fortunately be accurately modelled with extra effort, and instruments can be designed to handle a variety of different fuel types and geometries. [44, 45, 46]

Regardless of the difficulties, the laser flash method has been shown to be an excellent method for measuring the thermal conductivity of multiple fuel types under varying conditions. Determination of this property under different burnup conditions and temperature for fuel pellets is highly desirable since the fuel pellet itself generally provides the greatest resistance to the radial flow of heat, the increase of which could lead to melting. Additionally, the migration of volatile fission products such as Kr and Xe is temperature dependent, so knowing the temperature distribution during the fuel's operational life allows for the estimation of internal pressure in the fuel rod. If the clad integrity is breached, such knowledge of the gas distribution allows for the assessment of radiological consequences of their escape.

DSC

Differential Scanning Calorimetry (DSC) is a thermal technique that measures the difference in heat required to increase the temperature of a sample and reference as a function of temperature. For the duration of any given experiment, both are maintained at the same temperature, and the temperature is usually increased at a linear rate. Accurate measurements require that the reference have a well-defined heat capacity over the temperature range of interest. Different variations of this method exist such as Power Differential DSC and Temperature Modulated DSC (for specific heat), but all are rather useful for detecting and quantifying exothermic and endothermic phase transitions. This provides a more complete thermal profile of a bulk fuel mixture, which is important for determining safe burnup and fuel stability. A few examples are listed below.

This method has been frequently applied for the design of metallic and MOX fuels for fast breeder reactors. [47] In a mixed-metal fuel, the eutectic phase diagram generally isn't known, making DSC a superb tool for determining these phase boundaries and ultimately, stable fuels. For MOX fuels, this method has also been used to examine the effect of Ce, a major fission product in U and Pu. It has also been used to quantify the amount of hydrogen dissolved in the Zr-alloys used for nuclear fuel cladding, i.e., a way of monitoring the hydride effect. [48, 49]

3.5.2 Destructive Techniques

Puncture Test

Most commercial fuel rods are pressurized with He to aid in heat conduction from the fuel to the cladding, while also minimizing fuel-cladding interactions. However, internal pressure changes occur over time due to dimension changes and fission gas release (mostly Xe) from fuel pellets, creating the potential for leakage. It is therefore of great importance to measure the internal pressure of a fuel rod to assist in determining the safe lifetime of a fuel rod design. To date however, the only way of measuring the internal rod pressure is with the rod puncture test, which consists of measuring the internal pressure and volume of the fission gas from a hole punctured into the fuel rod. Internal void volume can also be extrapolated from such measurements. As expected, care must be taken to prevent leaking of the fission gases into the atmosphere, a problem which can usually be solved with the use of cold traps.

β-γ autoradiography

In addition to pressure changes, the products of fission gas release are also β and γ emitters. By combing the puncture test with a plate sensitive to these decay products, β-γ autoradiography can help paint a more complete picture of fission product distribution as it relates to the problem of fuel swelling. This is especially important at research facilities that need to search for potential problems with new fuels before commercial use. Such testing has been practically demonstrated in for the macrostructure examination of irradiated MOX and fast-reactor fuel pins. [50] [51] [52]

LA-ICPMS/SIMS

Just like its namesake, Laser ablation inductively coupled plasma mass spectrometry (LA-ICPMS) uses a laser to ablate solid materials to generate fine particles that are then analyzed with an integrated ICPMS. This is quite useful for mapping isotope distributions in nuclear fuel and shielding materials. [53] A specialized setup for radioactive samples has been described in the literature by Guillong, et al, who used the instrument to ablate UO_2 references. Isotope ratios were measured with a precision of 0.3%, detection limit of 0.1 ppm and a spatial resolution of to 20 µm. LA-ICPMS has especially been proven to be useful when combined with the rod puncture test, both to measure fission gas products and the pressure of individual gas bubbles (Xe/Kr) effusing on a µm scale. Isotopic fractions or the Xe/Kr ratio can be compared to fuels in various burnup stages in addition to a detailed history of the fuel as Pu builds up over time, which is useful information for proliferation efforts. However, explaining a particular distribution requires the use of complementary techniques such as XAFS, which can give local information that identifies nearest neighbors of the element in question. [54] [55]

As in FIB, in SIMS the sample surface is sputtered with Ga(I) ions, which can then be analyzed in a mass spectrometer via the production of secondary ions. It has been shown to have produce fast element imaging and depth resolution, excellent sensitivity for trace elements produced by fission, accurate isotopic measurements and capable of detecting gas bubbles. [56] This has been shown in a detailed review on the SIMS of irradiated nuclear fuels by Portier et al., who found that it is a powerful complement to EPMA. However, the signal is highly dependent on a variety of factors such as matrix effects (chemical environment), detector efficiency, and isobaric interferences. [57]

Optical Microscopy

Optical microscopy is a standard topological surface technique used for the micron-level examination of commercial fuel cladding materials. Phenomena studied include the formation and movement of grain boundaries, oxide layer formation, or even the morphology, distribution and orientation of Zr-hydrides, all

effects that could lead to structural failure. [58] This makes this technique highly useful for studying the evolution of these properties under a variety of simulated real-world conditions such as dry-cask storage and potential coolant loss. [59] For example, in the latter case, optical microscopy could be used to measure the thickness of inner and outer oxide layers formed by interactions of the metal-alloy with steam. Since it is known that these layers lower the ductility of the fuel cladding, measuring the thickness of these layers with under high-temperature reactor conditions should show if they are safe to use. [60] However, the preparation of these metal samples for optical microscopy are also responsible for the auxiliary facilities for the grinding, polishing, and etching of samples. Materials must be carefully prepared such that damage to the sample is minimized and serves as an accurate representation damage caused by reactor conditions. [61]

Mechanical Testing

Mechanical testing refers to a rather broad category of bulk material measurements made either for testing new materials, or as quality control for those with well-known mechanical properties. With regards to the nuclear industry, mechanical stress testing is important for determining if the fuel cladding can withstand the harsh, high-radiation and high temperature environment in a nuclear reactor, or to determine if a fuel assembly could be safely transported to a storage site after the fuel has been spent. For the sake of brevity, discussion here will be limited to Vickers hardness, tensile and burst testing. [62]

The Vickers hardness test is common for determining a materials resistance to plastic deformation. This is usually carried out with a hardness tester and has been integrated with optical microscopy to study the hardness and crack formation in new fuels, post irradiation and/or under thermal shock with a temperature-controlled furnace. The latter process usually dominates for the so-called in-reactor creep, which can produce structural weaknesses. These changes also occur on the sheath of a fuel rod, which is where tensile testing becomes important. [63]

This is so because the cladding-fuel interface provides the greatest chances of structural failure in a fuel rod. Additionally, highly spent fuel is especially vulnerable to the effects of hydride reorientation and can lead to embrittlement, greatly affecting how the rods can be safely transported or stored. [64] Experiments are performed in a variety of ways depending on the application, but generally refer to a test of stress vs strain under an elongated/compressive/shear load, with compressive tests often requiring a specialized load frame. Strain can be measured with the standard strain gauge or with a digital image correlation system, which uses high-definition images to measure deformation based on the displacement of a surface speckle pattern. [65]

Finally, burst testing is another important mechanical test commonly used for potential fuel rods. As has been mentioned before, Xe and Kr are fission products that migrate through the fuel and cladding at a rate that is temperature dependent. The goal of burst testing is to determine the maximum pressure at which the rod would fail and begin to leak. This is important for predicting safe operating temperatures and burnup in the nuclear fuel cycle. [66]

FIB

Focused Ion Beam (FIB) spectroscopy is like SEM, except a focused beam of ions is used instead of electrons, with Ga(I) being the most common. [67] However, this key difference makes use of this tool both versatile and selective. In this technique, liquid metal ion sources accelerate Ga through a pointed W needle with an applied energy of 1-50 keV, which is then focused onto the sample through a set of electrostatic lenses. The result of this operation is to sputter neutral atoms or ions of the material and SEs, which can be

detected and used to image a surface. At low applied currents, the image resolution has been shown to rival even SEM. [68]

Some of the advantages of FIB over SEM for nuclear materials is that when imaging SEs and ions, grain orientations contrast can be imaged very clearly. Additionally, secondary ions can reveal corrosion, as metal ion intensity increases in the presence of oxygen. [69] Often, FIB systems are combined with an electron beam column and used to prepare samples for SEM imaging, as has been done for UO_2 pellets. [70] In that particular case, the FIB was being used for its capability to machine layers via sputtering, while the SEM was used for imaging of separate layers. Curiously, McKinley et al. have shown how FIB can be used for tomography in irradiated materials, which essentially relies on specialized methods and algorithms for stitching 2D images to a 3D visualization of the microstructure. [71]

TGA

Thermal Gravimetric analysis (TGA) is a standard thermal technique used to monitor the change in sample mass with respect to temperature or time in a controlled atmosphere. In the case of nuclear fuels, the interest primarily lies is measuring the mass change as the temperature is increased to test fuel stability under high temperature conditions. For examples, it has been used to examine the safety of mixed-nitride fuels used in fast neutron reactors. These are generally known to possess high vapor pressures above 2100 K, leading to the undesirable migration of Pu and U to the cladding. [72] It has also been used to study the stability of studtite, which has been thought to form as a secondary solid phase on spent nuclear fuel, helping to determine its feasibility for long-term geological storage. [73]

4. Basic Neutron Science Facilities (BSFs)

4.1 Intro to BSFs

Basic Science Facilities (BSFs) comprise most RR facilities for any research program, and use neutrons for imaging, spallation, and spectroscopy. They should have no or minimal hot cells for material processing. For BSFs, the RR is used to give high flux beam through steady or pulsed operation. As beam neutrons directly relate to the core neutron flux, RR core flux is a good indication of the types of beam studies that can be performed with most beamlines requiring thermal flux from 1E14–1E15 n cm^{-2} s^{-1}. While the operational flux is similar to MIF requirements, the sample sizes are smaller.

Example BSF supporting facilities include Cold Neutron Research Facility (NIST) (Figure 4-1), the Advanced Neutron Source (ORNL), MURR (University of Missouri Research Reactor), MacClelan Nuclear Research Center, and the Thermal Neutron Beam Facility at Ohio State University.

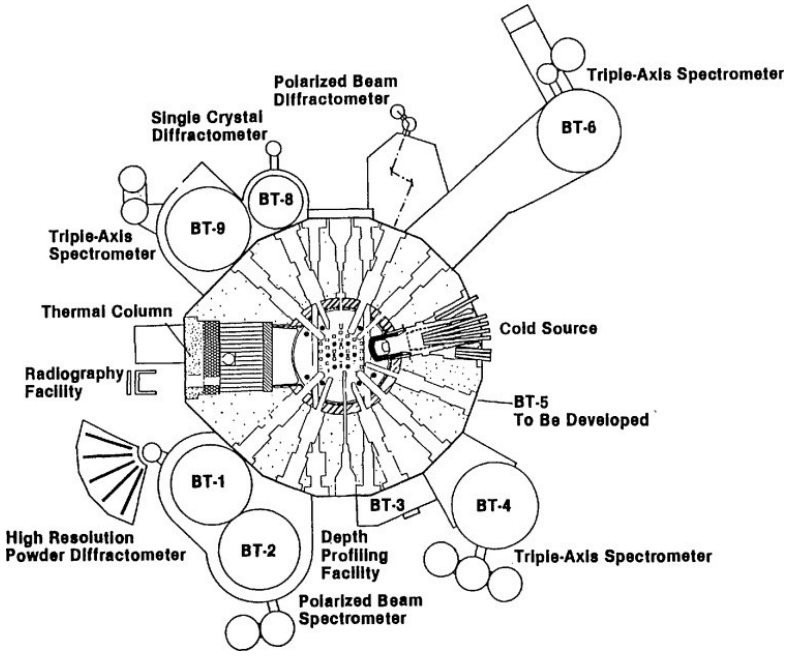

Figure 4-1: Experimental facilities for an example BSF (NIST Cold Neutron Research facility). [74]

4.2 Typical Attributes of BSFs

BSF beamlines support a variety of neutron experiments through beamlines. These methods include:

- Neutron gaging,
- Neutron diffraction (ND),
- Neutron imaging techniques (e.g., neutron radiography (NR), neutron radioscopy, neutron tomography and neutron based autoradiographic techniques),
- Prompt or capture gamma ray in beam neutron activation analysis (PGNAA, NCA),
- Neutron scattering (NS): elastic, inelastic and small angle neutron scattering (SANS),
- Neutron polarization,
- Neutron reflectometry,
- Neutron interferometry.

These methods will have distinct end detectors, but the beamlines used to guide the neutron beams all share common attributes.

4.3 Neutron Irradiation Positions and Associated Systems in BSFs

Beam ports are tubes that have been bored into the shielding of the reactor and are filled with air or an inert gas allow for neutrons to be emitted from the core of the reactor. Due to the straightforward set up of beam ports, both materials irradiation processes and neutron spectroscopy can be done using this neutron irradiation position and support system.

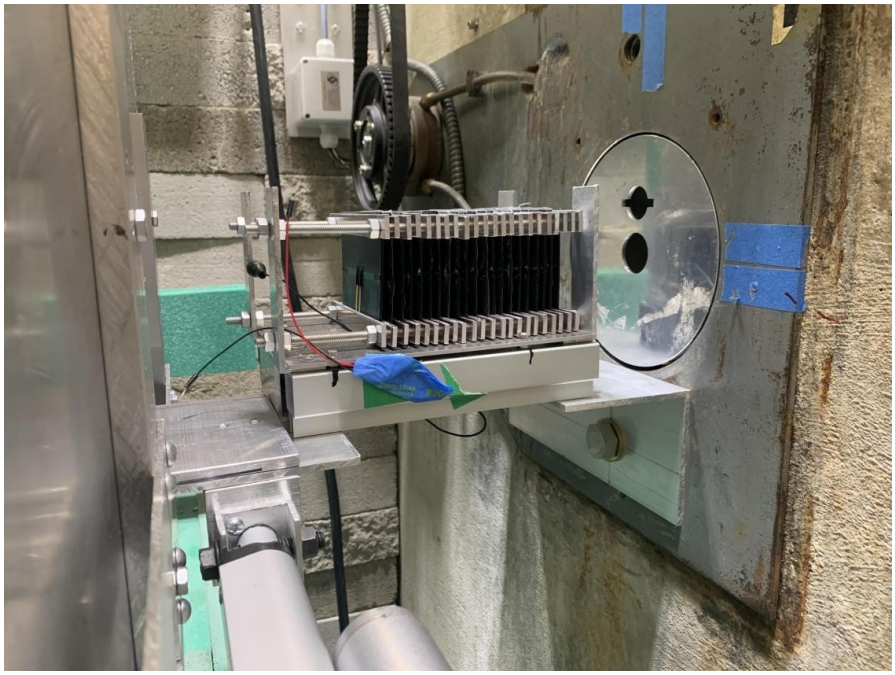

Figure 4-2: A beam port for a fast neutron beam at the Ohio State University Research Reactor. [75]

Beamlines can be used with fast neutrons or cold neutron systems. Fast neutron beamlines use neutrons that have not been moderated and thus keep their kinetic energy. This can also be done by creating a beamline from the core that sends thermal neutrons to uranium plates that fission and release fast neutrons. Fast neutrons, however, can cause a loss of contrast in radiographic films. This means that radial beamlines require filters and collimators to filter out fast neutrons and provide higher purity thermal neutron beams. Tangential beam lines reduce the required filters greatly and are preferable to radial beamlines due to the lower equipment costs.

Thermal neutron beamlines should have intensities much greater than 1E8 n cm^{-2} and have a diameter of at least 2 cm. Thermal beamlines should include their own collimator and the emitted beam should be able to cover the desired sampling area - either the entire sample or a representative section. Beams can be guided using a neutron wave guide which can be made from Si and Ti. Thermal neutron guides, including mirror guides, can be used to conduct the neutrons from the beam port to a region away from the background neutrons near the reactor. In many cases, the neutrons are conducted through a guide into a separate building adjacent to the reactor building. This process provides a major improvement in the signal to noise ratio (neutron signal to neutron background ratio). While guides are routinely utilized at high power level research reactors, they are especially useful for intermediate and lower power level reactors.

Some RRs utilize cold neutron sources, which give high intensity neutrons and low background. Cold neutrons have wavelengths longer than 4 Å, with these neutrons only counting for 1–2% of the total neutron flux in a normal distribution of a RR. Cold neutron sources can increase the cold neutron flux of a beam line by a factor of 20 – 40 and this amount and can increase the wavelength of a cold neutron beam by 5 Å. Obtaining an appropriate length to diameter ratio (L/D) for the set-up may require extension of the beam tube. It should be noted that the space requirement for the external portion of the set-up (specimen, converter, film station, shielding) is significant. [76]

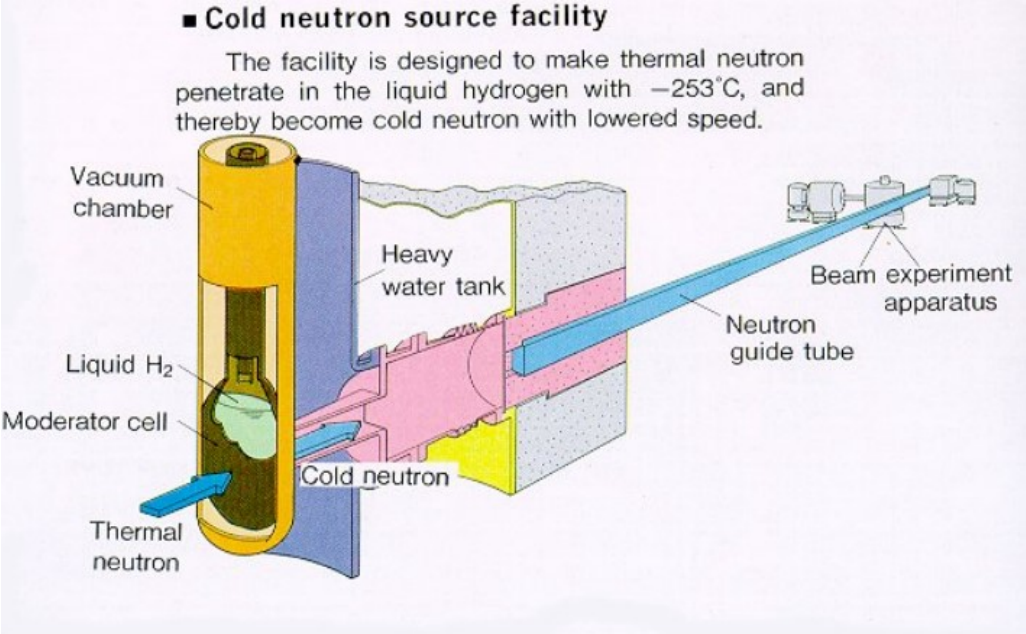

Figure 4-3: Example of a cold neutron system. [2]

Beamlines from RR support a variety of instrumentation for neutron optics. For example, MITR has two neutron scattering facilities. One facility has a triple-axis diffractometer equipped with PG monochromator, PG analyzer, He-3 monitors, and detector and standard collimators, slits, and PG filters, and another facility contains neutron optics test station with polychromatic neutron beam.

Many RR also have tandem accelerators that can be used for the generation of ions to interact with the neutrons. The Ion Beam Laboratory at the UMNR houses an NEC 1.7 MV tandem accelerator. The accelerator is actively used for research aimed at advancing the science of radiation damage of materials including alloys, ceramics, and coatings. The accelerator is equipped with TORVIS and SNICS ion sources for enhanced capabilities and the temperature of the samples is monitored by thermocouples and IR cameras. The systems are equipped with three beamlines with three chambers currently for different purposes of irradiations and in-situ measurements. The facility's capabilities are designed to meet the research needs of the scientific community involved in research on radiation damage of materials and other fundamental materials science research areas involving ion irradiation. The sample sizes are 2.3 cm^2, 1.5 cm^2, and 225 cm^2.

5. Proliferation Concerns and Opportunities

RR AUX facilities present a series of proliferation concerns due to how varied each facility is and how closely certain neutron irradiation position and associated systems such as rabbit tubes and test loops can replicate reactor conditions. MIFs use medium to higher powered reactors, making these facilities more desirable to proliferators. Materials being placed in test positions are often within the core or in high flux areas to readily absorb neutrons. If used with specific targets, such as depleted uranium (DU) or special nuclear material (SNM), a MIF could potentially be used to proliferate. To avoid this, MIF facilities should clearly define equipment being used in hot cells, avoid having excess space in hot cells for flexibility, and engineer rabbit tube capsule sizes that would be disadvantageous to using SNM within samples that can

enter high flux areas. Equipment found in hot cells of a declared MIF should not include isotope separations, with only packaging equipment detailed for use in conjunction with off-site facilities that can provide further analysis of an irradiated sample. Shielding for hot cells should not exceed more than 10% above the safety standards set for the type of declared activity being performed in the hot cell to prevent easy misuse of hot cell. This methodology can increase throughput of MIF-related activities. Readily defining an AUX facility's purpose before construction of the facility along with expected activities for the nuclear program can help inspection activities as well.

Some experiments performed in BSFs can utilize lower power reactors, though there are BSFs that host experiments that require high neutron flux (such as at HFIR). As with MIFs, designing beam lines and clearly stating the purpose of each experiment being carried out at the BSF will allow for control of equipment, flux at each beam line and assist with optimization of the layout of the facility. Each beam line should be reviewed to confirm that the flux and diameter of the beam is appropriate for the experiments being carried out at the beam line.

A cursory estimation of plutonium production capacity in irradiation facility pneumatic/hydraulic capsule systems, test loops, and beam ports has been performed as part of this survey using a neutronics model of a hypothetical 10 MW light water reactor. The modeled reactor featured a central flux trap simulated by an absent central fuel assembly replaced with a postulated depleted uranium target. Both metal and oxide compositions were evaluated as well as various target slug diameters to capture the effects that resonance self-shielding and density have on throughput.

The accessible irradiation positions available to a given facility will dictate the size and quantity of targets that can be irradiated and while a larger target would produce more plutonium than a smaller one, it does so with lower volumetric efficiency. Furthermore, larger targets can be significantly harder to adequately cool. Although thermal modeling is not in the scope of this survey, it is presumed that target locations larger than 2 cm in radius would likely require plate or annular target geometries to provide sufficient cooling if being exposed in medium or high-power reactors. Plate and annular fuels have higher production efficiency per gram of actual target material than the slugs analyzed in this effort, but obviously pack significantly less mass of target material in a given irradiation channel than do slugs.

Plutonium production estimates reported here assume a direct linear relationship with flux such that doubling the flux at the target location would double the plutonium production rate. This a realistic assumption with the only caveat being that higher flux leads to some additional neutron captures on the relatively short lived ^{239}Np, leading to very slightly higher ^{240}Pu content. The reactor model used in this estimation effort also assumes only a single, small slug being irradiated to yield a plutonium production rate normalized by volume. Were the proliferating operator to irradiate more than the single slug modeled, the available flux in core would decrease and the volumetric production rate would drop commensurately. The estimate given here is therefore considered bounding.

The results of depletion model of the hypothetical 10 MW reactor were used to track the plutonium isotopic composition in the targets over the course of several months. Figure 5-1 displays the weight fractions of each plutonium nuclide along with ^{239}Np, the precursor to ^{239}Pu, for the 1 cm radius metal DU slug case.

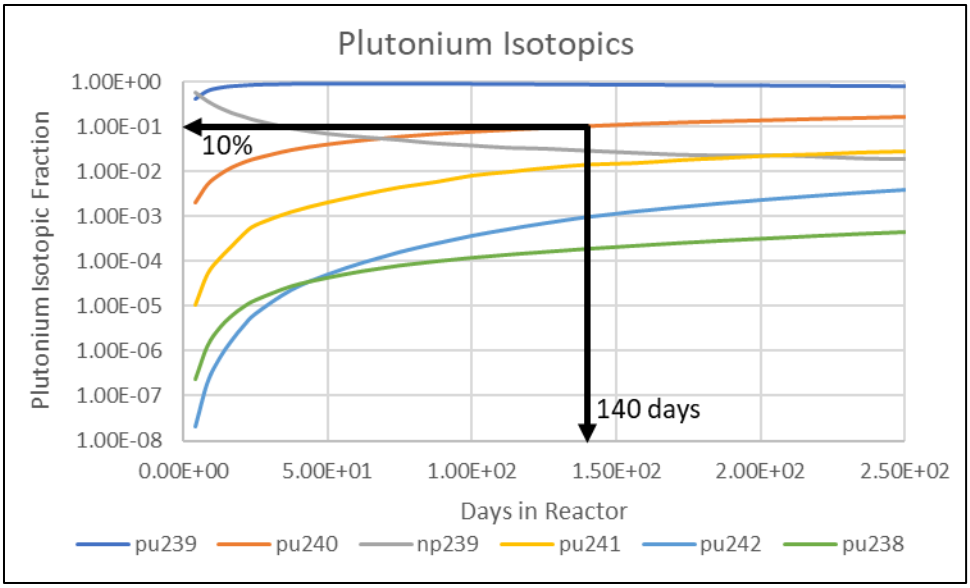

Figure 5-1: Plutonium isotopic fractions for a 1 cm radius DU metal slug

The time at which the ^{240}Pu fraction reaches 0.10 was used to determine a generalized rate of weapons grade plutonium (WGPu) production for each case. By normalizing this value by the calculated flux in an empty irradiation channel, one can estimate the bounding rate of production for pneumatic tubes, test loops, or beam ports of any given flux level. The results have been tabulated in Table 5-1 and plotted in Figure 5-2 for values of fluxes that could reasonably be expected to generate notable quantities of plutonium.

Table 5-1:Plutonium production estimates for slug DU targets

Target Description	Total flux in Empty Tube of 10 MW Reactor (n cm^{-2} s^{-1})	Target Volume (cm^3)	Days of Irradiation until 10%	WGPu Produced (g)	WGPu (g yr^{-1} cm^{-3})	WGPu (g yr^{-1} cm^{-3} per 1E12 n cm^{-2} s^{-1})
0.5cm Metal	1.86E14	7.85	91.0	1.5	0.7842	4.22E-03
1cm Metal	1.82E14	31.42	141.6	6.7	0.5533	f3.04E-03
2cm Metal	1.93E14	125.66	233.7	28.9	0.3597	1.86E-03
0.5cm Oxide	1.86E14	7.85	90.6	0.9	0.4401	2.37E-03
1cm Oxide	1.82E14	31.42	115.1	3.3	0.3367	1.85E-03
2cm Oxide	1.93E14	125.66	165.0	13.5	0.2378	1.23E-03

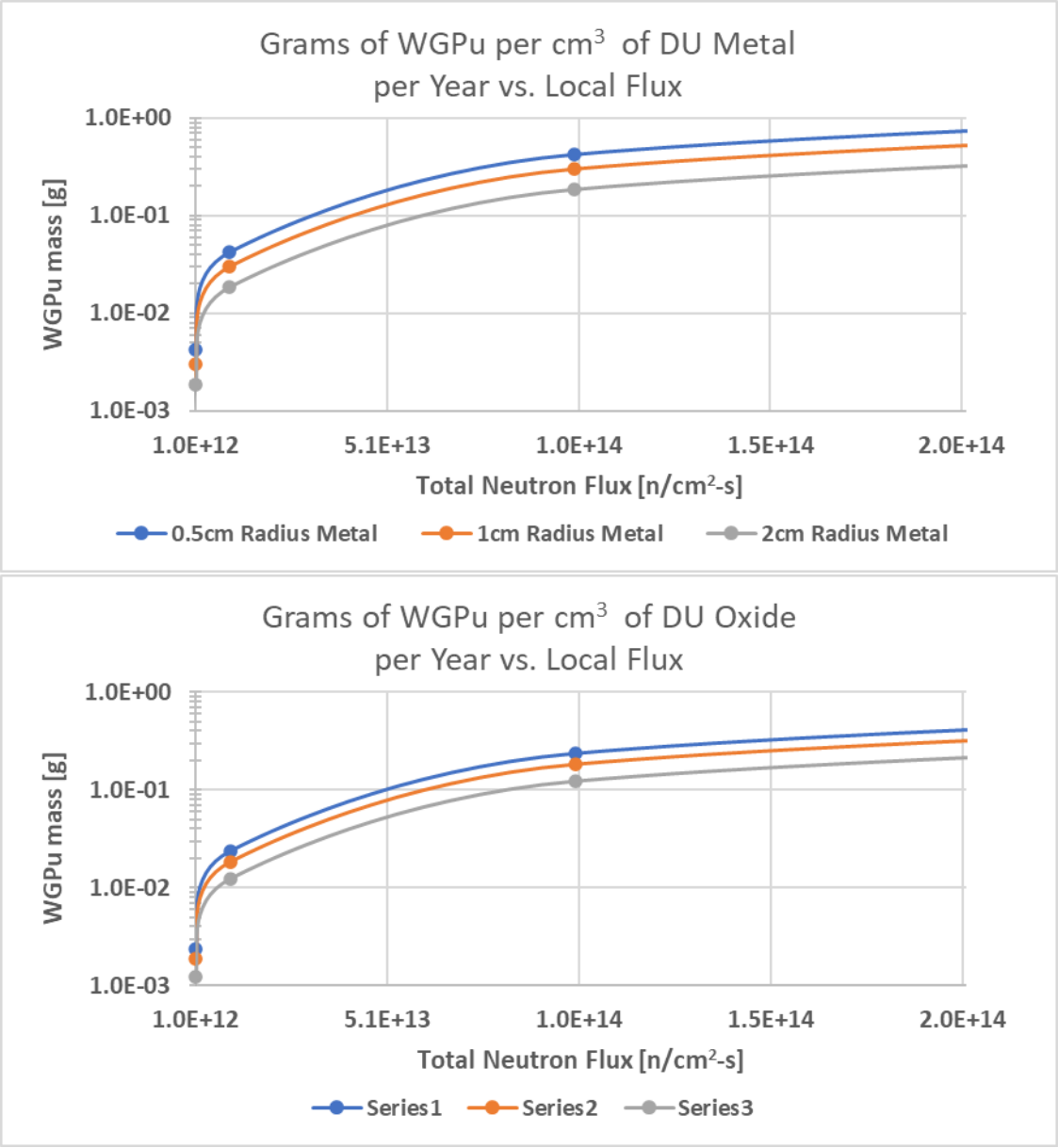

Figure 5-2: Weapons grade Plutonium (10% ^{240}Pu) production rate normalized by metal (top) and oxide (bottom) target volume

It may be concluded from these estimates that horizontal beam ports should not be expected to produce any concerning quantities of plutonium as they typically feature fluxes less than 1E10 n/cm^2-s. Capsule systems are somewhat limited in volume and may have cooling concerns, particularly in the case of pneumatically driven capsules, but they do at least provide flux levels that could likely yield tens to hundreds of grams of WGPu per year. Commercial facilities used for doping silicon or transmuting gemstones provide sufficient volume and flux to be of concern, but they do not inherently possess enough cooling to accommodate large scale plutonium production. Mechanical systems and test loops provide the most obvious irradiation systems for bulk plutonium production as they deliver targets to the heart of the reactor grid and utilize either the active cooling of the reactor or a separate dedicated cooling system that can be tuned as needed.

The estimates reported here do not reflect the optimal balance between plutonium production throughput and target thermal design, but they can be used to indicate the relative proliferation risks of a facility's material irradiation and test systems. Additional work may be considered to evaluate D_2O moderated or fast flux facilities.

6. Conclusions – Suggested PRO-X Next Steps for MIFs and BSFs

This survey focused on the potential application of PRO-X methodology to two generalized AUX facility types – the materials irradiation facility and the basic science facility. For the two facility types, typical neutron irradiation positions and associated systems were discussed along with neutron fluxes, sample size, and equipment sizes. In addition to the basic attributes associated with neutron irradiation systems, a surveyed list of active RRs and their associated parameters were included as they were available. This work was performed to provide a foundation for future partnerships in which the PRO-X team will work with RR operators, owners, and vendors to assess the impacts of potential design options for an optimized AUX facility. In addition to the survey, discussion on the potential for proliferation in each of these facility types was performed with some general parameters of neutron flux and material sizing to assist in determination of levels of concern for each neutron irradiation system.

Work in FY24 and beyond should focus on identification and classification of proliferation concerns in MIF and BSF type AUX facilities. This future work will focus on these efforts:

1. A model of projected throughput for different MIF and BSF configurations that will be used to provide a window of potential operational misuse for a facility and better understand the capability of production and the rate of processing for WUNM in these facilities.
2. A misuse study for various configurations of MIF hot cell layouts detailing capacity, specifications, shielding constraints for MIF operations, identification of a maximum shielding thickness, and reasonable need associated with each activity performed in a MIF.
3. Development of a rule of thumb rating system utilizing data gathered from previous reports to show levels of concern at a given power level, flux, and experiment set.

Future reporting detailing facility proliferation based on modeling demonstrated in this report and development of a rating system for assigning risk will provide a deep understanding of optimization and non-proliferation strategies that can be performed for future AUX facilities. This modeling will utilize methodology found in section 5 of this report to build windows of potential misuse by samples that could be included in irradiation positions for experimental activities and the risks of loading, unloading, and packaging of amount of WUNM produced. Further exploration on hot cells for MIFs will be required for assessing how to optimize these systems utilizing PRO-X methodology. Due to the nature of some facilities sharing operational space for different purposes, further review of RR AUX facilities should be conducted to gain a greater understanding of MIF hot cell configurations. These reports will lead into the creation of a classification system for level of proliferation concern based on the flux and power level of a reactor that is coupled with the experimental equipment and activities that are expected to be performed in a given AUX facility. This will provide an encyclopedia for the development of future proliferation-resistant MIF and BSF facilities.

7. References

[1] R. R. P. B. a. E. A. D. N. F. Greenberg, "Neutron activation analysis: a primary method of measurement," *Spectrochimica Acta Part B: Atomic Spectroscopy 66, no. 3-4,* pp. 193-241, 2011.

[2] International Atomic Energy Agency, "The Applications of Research Reactors," IAEA, Vienna, 4-7 October 1999.

[3] M. R.-S. J. W. A.-S. J. A.-S. J. M. M.-S. S. M. P.-S. a. A. S.-A. M A Brown-ANL, "Proliferation Resistance Optimization (PRO-X) Methodology to Evaluate Research Reactor Isotopic Production Auxiliary Facilities," U.S. Department of Energy, 2022.

[4] D. K. G. a. H. L. Carpenter, "MITR Users' Guide," Massachusetts Institute of Technology, Jul. 2012.

[5] International Atomic Energy Agency, "Neutron Transmutation Doping of Silicon at Research Reactors," International Atomic Energy Agency, Vienna, 2012.

[6] Nuclear Regulatory Commission, "ISSUANCE OF AMENDMENT NO. 6 TO FACILITY OPERATING LICENSE NO. R-110 - IDAHO STATE UNIVERSITY AGN-201M RESEARCH REACTOR (TAC NO. MB6757)," U.S. Nuclear Regulatory Commission, 2006.

[7] Nuclear Regulatory Commission, "Reactor Oversite Process," U.S. Nuclear Regulatory Commission, Washington, DC, 2016.

[8] S. B. Grover, "Irradiation Facilities at the Advanced Test Reactor (No. INL/CON-05-00907)," Idaho National Lab (INL), Idaho Falls, ID, 2005.

[9] M. P. S. a. L. I. Kim, "Estimation of future demand for neutron-transmutation-doped silicon caused by development of hybrid electric vehicle and its supply from research reactors," *IEEE 13th European Conference on Power Electronics and Applications,* pp. 1-10, 2009.

[10] Massachusetts Institute of Technology, "Post Irradiation Examination | MIT Nuclear Reactor Laboratory," [Online]. Available: https://nrl.mit.edu/facilities/post-irradiation-examination. [Accessed 20 3 2023].

[11] Fuel Cycle Research & Development, "Capabilities of Existing Hot Cell Facilities for the Examination of Used Nuclear Fuel – Summary Report," U.S. Department of Energy, 2011.

[12] B. M. N. P. Y. B. N. G. C. R. L. S. P. E. T. D. C. F. M. a. G. C. Marchand, "Xenon migration in UO2 under irradiation studied by SIMS profilometry," *Journal of nuclear materials,* vol. 440, no. 1-3, pp. 562-567, 2013.

[13] U. Flückiger, "A comparison between alpha autoradiography and some measured alpha emitting actinide profiles in a plutonium containing fuel," *Nuclear Instruments and Methods,* vol. 180, no. 1, pp. 157-163, 1981.

[14] T. K. K. F. M. S. G. C. L. R. C. a. K. M. Parsons-Davis, "Application of modern autoradiography to nuclear forensic analysis," *Forensic science international,* vol. 286, pp. 223-232, 2018.

[15] T. S. B. D. J. P. B. C. K. P. V. a. M. S. Rao, "Quantitative estimation of plutonium-rich areas in thorium-based MOX fuels using alpha autoradiography technique," *Radiation measurements,* vol. 36, no. 1-6, pp. 747-750, 2003.

[16] K. R. J. B. K. a. S. D. Devi, "Plutonium heterogeneity in MOX fuel: a quantitative analysis," *Journal of Nuclear Materials,* vol. 518, pp. 129-139, 2019.

[17] J. P. J. a. R. P. Ghosh, "Use of autoradiography for checking plutonium enrichment and agglomerates in mixed-oxide fuel pellets inside welded fuel pins," *NDT International,* vol. 17, no. 5, pp. 269-271, 1984.

[18] C. S. D. P. A. M. A. A. M. P. J. a. K. H. Baghra, "Characterization and property evaluation of (Th–3.75 U) O2+ x fuel pellets fabricated by impregnated agglomerate pelletization (IAP) process," *Nuclear Engineering and Design,* vol. 259, pp. 113-117, 2013.

[19] C. S. D. S. J. W. N. B. P. A. M. a. K. A. Baghra, "Evaluation of micro-homogeneity in plutonium based nuclear reactor fuel pellets by alpha-autoradiography technique," *Journal of Nuclear Materials,* vol. 467, pp. 730-741, 2015.

[20] A. I. R. M. V. a. N. M. Loose, "Application of autoradiographic techniques for diffusion studies of nuclear fuel," *International Journal of Radiation Applications and Instrumentation. Part D. Nuclear Tracks and Radiation Measurements,* vol. 12, no. 1-6, pp. 945-947, 1986.

[21] K. R. J. S. A. S. P. D. J. S. I. a. C. S. Vrinda Devi, "Characterisation of nuclear fuel by spectroscopic evaluation of alpha autoradiographs," *Journal of Radioanalytical and Nuclear Chemistry,* vol. 314, no. 1, pp. 259-271, 2017.

[22] S. a. F. J. Caruso, "Design, development and utilisation of a tomography station for γ-ray emission and transmission analyses of light water reactor spent fuel rods," *Progress in Nuclear Energy ,* vol. 72, pp. 49-54, 2014.

[23] D. a. T. P. Jädernäs, "Electron Backscatter Diffraction of Nuclear Materials," *Microscopy and Microanalysis,* vol. 20, no. S3, pp. 1804-1805, 2014.

[24] Y. E. L. S. V. a. B. T. Goncharenko, "Possibilities and Features of Electron Backscatter Diffraction for Reactor Materials Investigation," in *AEA-HOTLAB Technical Meeting on Hot Cell Post-Irradiation Examination and Poolside Inspection of Nuclear Fuel*, Smolenice (Slovakia), 2013.

[25] V. Randle, "Electron backscatter diffraction: Strategies for reliable data acquisition and processing," *Materials characterization,* vol. 60, no. 9, pp. 913-922, 2009.

[26] T. T. T. W. A. S. C. S. K. a. A. A. Ajantiwalay, "Best practices for preparing radioactive specimens for EBSD analysis," *Micron,* vol. 118, pp. 1-8, 2019.

[27] J. A. Turnbull, "The effect of grain size on the swelling and gas release properties of UO2 during irradiation," *Journal of Nuclear Materials,* vol. 50, no. 1, pp. 62-68, 1974.

[28] D. R. V. F. J. K. A. E. L. W. D. a. S. K. Cui, "Characterization of alloy particles extracted from spent nuclear fuel," *Journal of nuclear materials,* vol. 420, no. 1-3, pp. 328-333, 2012.

[29] D. L. Y. Y. T. J. S. Z. Y. W. L. L. M. C. Z. a. S. W. Yang, "Application of binary Ga–Al alloy cathode in U separation from Ce: The possibility in pyroprocessing of spent nuclear fuel," *Electrochimica Acta,* vol. 353, p. 136449, 2020.

[30] V. J. C. D. W. L. B. V. J. G. M. S. T. F. a. M. C. Kerleguer, "The mechanisms of alteration of a homogeneous U0. 73Pu0. 27O2 MOx fuel under alpha radiolysis of water," *Journal of Nuclear Materials,* vol. 529, p. 151920, 2020.

[31] T. S. C. a. S. A. Roy, "Pressureless sintering of boron carbide," *Ceramics international,* vol. 32, no. 3, pp. 227-233, 2006.

[32] Y. L. W. D. C. a. A. T. Yang, "Stoichiometry effect on the irradiation response in the microstructure of zirconium carbides," *Journal of Nuclear Materials,* vol. 454, no. 1-3, pp. 130-135, 2014.

[33] C. Walker, "Electron probe microanalysis of irradiated nuclear fuel: An overview," *Journal of Analytical Atomic Spectrometry,* vol. 14, no. 3, pp. 447-454, 1999.

[34] J. D. L. V. C. N. J. B. T. R. I. a. P. B. Lamontagne, "Fission gas bubbles characterisation in irradiated UO 2 fuel by SEM, EPMA and SIMS," *Microchimica Acta,* vol. 155, pp. 183-187, 2006.

[35] C. D. C. K. G. B. J. a. B. C. Mieszczynski, "Investigation of irradiated uranium-plutonium mixed oxide fuel by synchrotron based micro X-ray diffraction," *Progress in Nuclear Energy,* vol. 57, pp. 130-137, 2012.

[36] C. M. M. K. G. G. D. a. B. C. Degueldre, "Plutonium–uranium mixed oxide characterization by coupling micro-X-ray diffraction and absorption investigations," *Journal of nuclear materials,* vol. 416, no. 1-2, pp. 142-150, 2011.

[37] J. a. P. D. Spino, "Lattice parameter changes associated with the rim-structure formation in high burn-up UO2 fuels by micro X-ray diffraction," *Journal of nuclear materials,* vol. 281, no. 2-3, pp. 146-162, 2000.

[38] C. T. L. M. P. a. D. D. Worley, "Application of micro-XRF for nuclear materials characterization and problem solving," *Powder Diffraction,* vol. 28, no. 2, pp. 127-131, 2013.

[39] E. F.-Z. A. M. M. B. A. G.-L. I. P. A. J. D. R. O. G. D. B. C. a. V. A. Curti, "X-ray absorption spectroscopy of selenium in high-burnup UO2 spent fuel from the Leibstadt and Oskarshamn-3 reactors," in *Final Workshop Proceedings of the Collaborative Project „Fast/Instant Release of Safety Relevant Radionuclides from Spent Nuclear Fuel*, 2016.

[40] M. Denecke, "X-Ray Spectroscopy in Studies of the Nuclear Fuel Cycle," *X-Ray Absorption and X-Ray Emission Spectroscopy: Theory and Applications,* pp. 523-559, 2016.

[41] A. W. D. O. M. C. D. W. W. P. G. a. S. A. Craft, "Neutron radiography of irradiated nuclear fuel at Idaho National Laboratory," *Physics Procedia,* vol. 69, pp. 483-490, 2015.

[42] W. J. R. B. C. a. A. G. Parker, "Flash method of determining thermal diffusivity, heat capacity, and thermal conductivity," *Journal of applied physics,* vol. 32, no. 9, pp. 1679-1684, 1961.

[43] J. W. C. S. D. P. D. a. Y. S. Turnbull, "Effect of Burn-up on the Thermal Conductivity of Light Water Reactor Fuel: Results of Investigations Employing the Laser Flash Technique," *Journal of Nuclear Materials,* p. 154398, 2023.

[44] M. D. C. a. T. P. Pouchon, "Determination of the thermal conductivity in zirconia based inert matrix nuclear fuel by oscillating differential scanning calorimetry and laser flash," *Thermochimica acta,* vol. 323, no. 1-2, pp. 109-121, 1998.

[45] Y. Philipponneau, "Thermal conductivity of (U, Pu) O2− x mixed oxide fuel," *Journal of nuclear materials,* vol. 188, pp. 194-197, 1992.

[46] M. H. D. M. M. a. R. C. Sheindlin, "Advances in the use of laser-flash techniques for thermal diffusivity measurement," *Review of scientific instruments,* vol. 69, no. 3, pp. 1426-1436, 1998.

[47] R. R. S. R. A. S. N. a. S. S. Santhosh, "Differential Scanning Calorimetry Study of U–Cr Alloys," *Transactions of the Indian Institute of Metals,* vol. 68, pp. 305-308, 2015.

[48] K. a. I. S. Une, "Terminal solid solubility of hydrogen in unalloyed zirconium by differential scanning calorimetry," *Journal of Nuclear Science and Technology,* vol. 41, no. 9, pp. 949-952, 2004.

[49] R. a. M. M. Marinescu, "Hydrogen concentration determination in pressure tube samples using differential scanning calorimetry (dsc)," Interantional Atomic Energy Agency, 2015.

[50] G. a. T. G. Pugnetti, "Application of alpha and beta-gamma autoradiography in shielded cells for the examination of irradiated nuclear fuels," *Comitato Nazionale per l'Energia Nucleare,* pp. No. CNEN-RT/MET-71-1, 1971.

[51] D. a. T. H. Porter, "Full-length U–xPu–10Zr (x= 0, 8, 19 wt.%) fast reactor fuel test in FFTF," *Journal of nuclear materials,* vol. 427, no. 1-3, pp. 46-57, 2012.

[52] D. V. U. R. E. U. K. a. A. S. Sah, "Post irradiation examination of thermal reactor fuels," *Journal of Nuclear Materials,* vol. 383, no. 1-2, pp. 45-53, 2008.

[53] C. D. L. M. F. P. K. H. B. G. D. a. G. W. Kurta, "Rapid screening of boron isotope ratios in nuclear shielding materials by LA-ICPMS–a comparison of two different instrumental setups," *Journal of Analytical Atomic Spectrometry,* vol. 29, no. 1, pp. 185-192, 2014.

[54] M. H. P. K. Z. G. D. a. G.-L. I. Guillong, "A laser ablation system for the analysis of radioactive samples using inductively coupled plasma mass spectrometry," *Journal of Analytical Atomic Spectrometry,* vol. 22, no. 4, pp. 399-402, 2007.

[55] C. B. J. a. M. M. Degueldre, "Post irradiation examination of nuclear fuel: Toward a complete analysis," *Progress in Nuclear Energy,* vol. 92, pp. 242-253, 2016.

[56] J. N. J. D. L. B. T. P. B. a. R. I. Lamontagne, "Detection of Gas Bubble by SIMS in Irradiated Nuclear Fuel," *Microchimica Acta,* vol. 145, 2004.

[57] S. B. S. a. W. C. Portier, "Secondary ion mass spectrometry of irradiated nuclear fuel and cladding: An overview," *International Journal of Mass Spectrometry,* vol. 263, no. 2-3, pp. 113-126, 2007.

[58] K. U. K. H. M. I. K. a. S. Y. Nogita, " Effect of grain size on recrystallization in high burnup fuel pellets," *Journal of nuclear materials,* vol. 248, pp. 196-203, 1997.

[59] K. T. Moore, "X-ray and electron microscopy of actinide materials," *Micron,* vol. 41, no. 4, pp. 336-358, 2010.

[60] H. S. R. a. B. M. Chung, "Characteristics of hydride precipitation and reorientation in spent-fuel cladding No. ANL/ET/CP-103367," Argonne National Lab, 2000.

[61] L. D. L. F. a. H. J. Capriotti, "Testing fast reactor fuels in a thermal reactor: Comparison of transmutation metallic fuel alloys behavior by scanning electron microscopy," *Journal of Nuclear Materials,* vol. 575, p. 154221, 2023.

[62] K. K. T. R. E. a. H. X. Metzger, "Determination of mechanical behavior of U3Si2 nuclear fuel by microindentation method," *Progress in Nuclear Energy,* vol. 99, pp. 147-154, 2017.

[63] Y. L. S. K. H. J. C. a. D. C. Lee, " Study on the mechanical properties and thermal conductivity of silicon carbide-, zirconia-and magnesia aluminate-based simulated inert matrix nuclear fuel materials after cyclic thermal shock," *Journal of nuclear materials,* vol. 319, pp. 15-23, 2003.

[64] J. a. W. H. Wang, "Mechanical Fatigue Testing of High Burnup Fuel for Transportation Applications No. ORNL/TM-2014/214," Oak Ridge National Lab, High Temperature Materials Lab, Oak Ridge, TN, 2015.

[65] T. S. H. C. X. K. T. G. J. K. Y. a. T. H. Nozawa, "Non-contact strain evaluation for miniature tensile specimens of neutron-irradiated F82H by digital image correlation," *Fusion Engineering and Design,* vol. 157, p. 111663, 2020.

[66] Z. R. W. G. B. E. L. a. J. M. Yanwei, "Burst Test Research on Zirconium Alloy for Nuclear Fuel Cladding Tubes," *Rare Metal Materials and Engineering,* vol. 46, no. 6, pp. 1491-1496, 2017.

[67] A. M. J. M. B. a. C. J. Aitkaliyeva, "Implementation of focused ion beam (FIB) system in characterization of nuclear fuels and materials," *Micron,* vol. 67, pp. 65-73, 2014.

[68] J. S. L. a. U. M. Orloff, "Fundamental limits to imaging resolution for focused ion beams," *Journal of Vacuum Science & Technology B: Microelectronics and Nanometer Structures Processing, Measurement, and Phenomena,* vol. 14, no. 6, pp. 3759-3763, 1996.

[69] L. A. P. K. L. K. J. A. D. K. L. J. M. J. Š. R. a. K. I. Celbová, "Diamond Coating Reduces Nuclear Fuel Rod Corrosion at Accidental Temperatures: The Role of Surface Electrochemistry and Semiconductivity," *Materials,* vol. 14, no. 2, p. 6315, 2021.

[70] J. Z.-A. I. a. B. T. Noirot, "Focused ion beam–scanning electron microscope examination of high burn-up UO2 in the center of a pellet," *Nuclear Engineering and Technology,* vol. 50, no. 2, pp. 259-267, 2018.

[71] C. S. C. H. G. G. T. a. A. A. McKinney, "A practical guide to characterizing irradiated nuclear fuels using FIB tomography," *Micron,* vol. 158, p. 103290, 2022.

[72] M. K. G. T. A. D. A. S. M. S. I. M. N. U. E. a. C. V. Krivov, "Thermogravimetric study of mixed uranium-plutonium fuel for prospective generation IV reactors," *Journal of Nuclear Materials,* vol. 567, p. 153798, 2022.

[73] A. C. I. G. J. Q. J. a. D. P. J. Rey, "Effect of temperature on studtite stability: Thermogravimetry and differential scanning calorimetry investigations," *Journal of nuclear materials,* vol. 385, no. 2, pp. 467-473, 2009.

[74] H. J. J. M. R. J. J. R. a. I. G. S. Prask, "The NIST cold neutron research facility," *Journal of research of the National Institute of Standards and Technology,* p. 98 no. 1, 1993.

[75] Ohio State University, "Nuclear Reactor Laboratory," [Online]. Available: https://reactor.osu.edu/fast-neutron-beam-facility. [Accessed 3 April 2023].

[76] International Atomic Energy Agency, "Use of neutron beams for low and medium flux research reactors: radiography and materials characterization: Report of a Technical Committee Meeting held in Vienna," International Atomic Energy Agency, Vienna, 4-7 May 1993.

[77] N. C. B. C. J. D. C. D. I. N. O. C. H. a. S. S. Woolstenhulme, "Development of irradiation test devices for transient testing," *Nuclear Technology,* 2019.

[78] A. F. Rowcliffe, "Neutron irradiation facilities for fission and fusion reactor materials studies," *Nuclear Instruments and Methods in Physics Research Section A: Accelerators, Spectrometers, Detectors and Associated Equipment 249, no. 1,* pp. 29-33, 1986.

[79] D. Morrell, "2012 Annual Report Research Reactor Infrastructure Program (No. INL/EXT-12-27816)," Idaho National Lab (INL), Idaho Falls, ID, 2012.

[80] C. Y. E. Park, "AFCF Existing Facilities Data Report (GNEP-AFCF-PMO-AI-EA-2008-000205)," Department of Energy, 2008.

[81] C. C. M. A. J. a. B. H. Jensen, "In-depth thermal-conductivity profile of ion-irradiated zirconium carbide using scanning thermal microscopy," *International Journal of Thermophysics,* vol. 34, no. 4, pp. 597-608, 2013.

[82] S. a. M. T. Hayden, "Fluorescent scanning thermal microscope based on a Blu-ray optical head to measure thermal diffusivity of radioactive samples," *Review of Scientific Instruments,* vol. 90, no. 2, p. 024903, 2019.

[83] Y. M. B. H. J. S. D. C. L. a. Y. T. Wang, "Transmission electron microscopy characterization of the fuel-cladding chemical interactions in HT9 cladded U-10Zr fuel," *Journal of Nuclear Materials,* vol. 572, p. 153990, 2022.

[84] T. L. X. W. Y. T. F. M. D. M. M. B. M. a. C. L. Yao, "ransmission Electron Microscopy based Characterization of a U-20Pu-10Zr Fuel Irradiated in Experimental Breeder Reactor-II," *Journal of Nuclear Materials,* vol. 568, p. 153846, 2022.

[85] T. K. M. R. I. W. T. T. H. P. D. a. R. V. Sonoda, "ransmission electron microscopy observation on irradiation-induced microstructural evolution in high burn-up UO2 disk fuel," *Nuclear Instruments and Methods in Physics Research Section B: Beam Interactions with Materials and Atoms,* vol. 191, no. 1-4, pp. 622-628, 2002.

[86] B. G. J. M. J. J. J. R. A. a. K. J. D. Miller, "Advantages and disadvantages of using a focused ion beam to prepare TEM samples from irradiated U–10Mo monolithic nuclear fuel," *Journal of nuclear materials,* vol. 424, no. 1-3, pp. 38-42, 2012.